Methods and models for the investigation of the uptake of Nanoparticles into hair follicles

DISSERTATION

zur Erlangung des Grades

des Doktors der Naturwissenschaften der

Naturwissenschaftlich-Technischen Fakultät III

Chemie, Pharmazie, Bio- und Werkstoffwissenschaften

der Universität des Saarlandes

von

Anne Susanne Raber

Saarbrücken

2014

Tag des Kolloquiums:	18.12.2014
Dekan:	Professor Dr.-Ing. Dirk Bähre
Berichterstatter:	Professor Dr. Claus-Michael Lehr
	Professor Dr. Thomas Vogt
Vorsitz:	Professor Dr. Uli Kazmaier
Akademischer Mitarbeiter:	Dr. Martin Frotscher

Ohne Begeisterung schlafen die besten Kräfte unseres Gemütes.

Es ist ein Zunder in uns, der Funken will.

Johann Gottfried von Herder

INHALTSVERZEICHNIS

SHORT SUMMARY

In this thesis in vitro skin models and methods were established to investigate the follicular uptake of nanoparticles (NP), especially quantitatively to estimate their potential for the transfollicular vaccination approach. To figure the amount of NP that can be deposited into the hair follicles a method was developed to quantify the follicular uptake of NPs. Comparing the results found in vitro in the pig ear model with the situation in vivo in human forearms an excellent in vitro in vivo correlation between both models was demonstrated, supporting the pig ear as surrogate for the situation in vivo.

To optimize the penetration efficiency of nanoparticles surface modifications were investigated as well as application techniques. The presence of different phospholipid coatings on the surface of poly(lactide-co-glycolide) (PLGA) NPs modulated the quantity of their penetration into the hair follicles. Massage is known to enhance the follicular penetration depth of applied NPs. However it was observed that massage cannot enhance the amount of NPs that penetrate the hair follicle.

In a proof of concept study, PLGA and chitosan-PLGA NPs were prepared with ovalbumin (OVA) as model antigen. In a cell culture assay CD4+ and CD8+ T-cells were stimulated by encapsulated OVA to a larger extent than by OVA in solution. An adoptive transfer experiment in mice confirmed the possibility of transfollicular vaccination without previous treatment of the skin.

KURZZUSAMMENFASSUNG

In dieser Arbeit wurden in vitro Hautmodelle und Methoden zur Untersuchung, insbesondere der quantitativen, follikulären Aufnahme von Nanopartikeln (NP) entwickelt um deren Eignung für die transfollikuläre Vakzinierung zu untersuchen.

Es wurde eine Quantifikationsmethode entwickelt, um die Menge an NP zu bestimmen, die im Haarfollikel deponiert wird. Zwischen den Ergebnissen mit dem Schweineohr als in vitro-Modell und dem Unterarm von Probanden in vivo besteht eine hervorragende in vitro–in vivo-Korrelation, welche die Eignung des Schweineohrs als Surrogat für die Situation in vivo belegt.

Um die Effektivität der Penetration in die Haarfollikel zu optimieren, wurde untersucht welchen Einfluss Oberflächenmodifikationen am NP und die Anwendung spezieller Auftragetechniken haben. So sind Überzüge aus verschiedenen Phospholipiden in der Lage das Ausmaß der Penetration von NP aus Polylactid-co-Glycolid (PLGA) zu modulieren. Es ist bekannt, dass NP tiefer in die Haarfollikel eindringen, wenn sie in die Haut einmassiert wurden. Jedoch vermag Massage nicht die Menge im Haarfollikel zu steigern.

Für eine Machbarkeitsstudie wurden PLGA und Chitosan-PLGA NP mit Ovalbumin als Modellantigen beladen hergestellt. Im Zellkulturversuch wurden CD4+- und CD8+-T-Zellen durch Ovalbumin beladenen Partikel stärker stimuliert als durch eine Ovalbumin-Lösung. Beim adoptiven Zelltransfer im Mausmodel konnte bestätigt werden, dass die transfollikuläre Vakzinierung ohne Vorbehandlung der Haut möglich ist.

1. INTRODUCTION

Parts of this chapter have been published in:

A. Mittal[#], A. S. Raber[#] and S. Hansen Particle based vaccine formulations for transcutaneous immunization Human Vaccines and Immunotherapeutics 9 (2013) 1950 - 1955

# the autors contributed equally to this work

The author of the thesis made the following contributions to the publication:

Planned an designed the manuscript, interpreted and wrote the chapters concerning absorption routes of nanoparticles applied to the skin and faciliated absorption methods along with introduction and conclusion.

1.1. INTRODUCTION

Infectious diseases impose a serious threat to public health worldwide. Among the strategies to fight infections only vaccination has the potential to eradicate the disease (the World Health Organization, WHO, certified the eradication of smallpox in 1979). New, safe, efficient, and cheap vaccination strategies are desperately needed to meet the needs of a growing population in developing countries as well as the challenges of fast spreading infectious diseases due to global traffic (e.g. 2009 swine flu pandemics).

Particle based vaccine formulations for trans cutaneous immunization (TCI) address several key issues in vaccination today. First of all TCI has been shown to induce superior immune responses as compared to systemic vaccines and to hold the potential to convey mucosal immunity. This is highly desirable to prevent microbial pathogens from entering the body through mucosal surfaces and thus block disease at a very early stage. This will also help to reduce the risk of horizontal transmission from infected individuals to susceptible hosts.

Many of the current strategies for TCI (e.g. micro-needles, Gene gun, PowderJect, skin abrasion), reduce the protective stratum corneum (SC) barrier for a significant time to facilitate the absorption of the vaccine. This makes them suboptimal for mass vaccination campaigns under critical hygienic conditions. Particle based formulations are an interesting alternative to this. Needle free strategies are at the forefront to combat vaccination-related transmitted diseases due to sharing of needles or needle stick accidents.

Over the past decade, particulate carriers have emerged as an attractive delivery strategy for antigens and adjuvants. Particle based formulations combine several desirable aspects which make them very attractive for antigen encapsulation. Vaccine antigens are often difficult biological entities, including

DNA, peptides, proteins, attenuated viruses, microorganism fragments. (Nano)encapsulation can improve the stability, facilitate absorption and also increase antigenicity by mimicking the size of microorganisms.

The co-delivery of adjuvants is tantamount to increase the immunogenicity of the antigen and may allow a reduction of the antigen dose. In the context of vaccination so-called dose sparing allows reaching more people when limited amount of vaccine antigen is available such as in global pandemics. Furthermore, vaccines with higher efficiency are also needed to enable protection of immunosuppressed and elderly patients. Importantly, by choosing the right adjuvant it is possible to polarize the immune response in a predetermined direction and convey mucosal immunity.

However, until now TCI using particle based vaccine formulations has made no impact on medical practice. One of the main difficulties is that nanoparticles (NPs) cannot penetrate the skin to an extent that would allow the application of the required dose of antigen. This is due to the formidable SC barrier, the limited amount of antigen in the formulation and often an insufficient immunogenicity. A multitude of strategies are currently under investigation to overcome these issues. We highlight selected methods presenting a spectrum of solutions ranging from transfollicular delivery, to devices disrupting the SC barrier and the combination of particle based vaccines with adjuvants discussing their advantages and shortcomings. Some of these are currently at an experimental state while others are already in clinical testing. All methods have been shown to be capable of transcutaneous antigen delivery.

1.3 ABSORPTION ROUTES TO NP APPLIED TO THE SKIN

One of the main challenges in TCI is that the vaccine antigens need to overcome the SC barrier in order to reach the Langerhans cells (LCs) in the epidermis which act as antigen presenting cells (APCs). Intact human skin is widely impermeable to solid NPs and microparticles (MPs). Ultra-flexible liposomes are an exception to this rule. Due to the addition of edge activators such as surfactants and/or ethanol they are able to change shape and squeeze through the lipid channels of the SC, supposedly following an osmotic gradient. [1, 2] Ultra-flexible liposomes have been used foremost for encapsulating protein antigens. [3, 4] By including positively charged lipids in the formulation they become amenable to complexing nucleotide based drugs and thus may be an alternative for DNA vaccination. [5-7] For a more extensive overview the reader is referred to some recent reviews. [8, 9] Furthermore, ultra-small NPs with sizes less than 10 nm can enter the SC to a low and highly variable extent. [10] The toxicity and lack of biodegradability of quantum dots, metal or metal oxide NPs notwithstanding, ultra-small NPs are not suitable for drug delivery and vaccination purposes due to the extremely small amount of drug or antigen which can be loaded onto these particles. Also due to their low and variable degree of penetration such formulations would probably require some active means of penetration enhancement to enable delivery of a suitable dose.

1.4 NP FOR TRANSCUTANEOUS VACCINATION

Polymeric NPs as well as lipid carriers which are often in the size range of a few 100 nm are especially interesting delivery systems for the purpose of TCI. Nonflexible NPs which are applied onto the skin migrate into the hair follicle openings by a size-selective mechanism (Figure 1a). [11] The hair follicle is a promising target for TCI without compromising the skin barrier. [12] Interestingly, the trans-follicular

route is a common pathway for the invasion of allergens such as pollen grains. [13] First evidence for the importance of the transfollicular route for transcutaneous vaccine delivery came from differences observed between hairy and nude mice. [14] At least for DNA vaccines the hair cycle state also seems to determine the successful transfection. [15] Inside the hair follicles antigen uptake by the rich pool of peri-follicular APCs is facilitated due to the absence of a SC barrier in the lower follicular orifice. [16] Therefore this delivery strategy does not require application of any further measures which would reduce the skin barrier. It seems that transfollicular delivery elicits a CD8+ biased response which is recommendable for combating intracellular microbes and developing vaccines against cancer and virus infections. [17] We showed that transfollicular delivery of the nano-encapsulated model antigen ovalbumin (OVA) elicited similar proliferation of OVA specific CD4+ T cells as an i.m. injection of the same dose of soluble antigen in an adoptive transfer model. [12] Nano-encapsulation into polymeric NPs improved the delivery of OVA into the hair follicles on excised pig ears by a factor of 2.5-3 compared to OVA in solution and protected OVA from cleavage or aggregation so that it maintained its biological activity to a high degree during storage and shipping. [12] As an important outcome of the study we observed in vitro as well as in vivo an intrinsic adjuvanticity of the NPs which was also influenced by the polymer material used. [12] The effect can probably be enhanced and directed by the combination or co-encapsulation of adjuvants into the formulation. As hair follicles cover only 0.1% of the skin surface trans-follicular delivery has long been discussed to be negligible. It was demonstrated however that the capacity of hair follicles is similar to that of the SC. [18] Lademann et al showed that NPs penetrated more efficient into the hair follicles than solutions and form a depot in the follicle that persists for more than one week. [19] Still a big issue with transfollicular application is the loss of formulation on the skin surface. Consequently a higher amount of vaccine would be required to achieve delivery of the required dose, which will need to be optimized in the future to make transfollicular vaccination a real alternative.

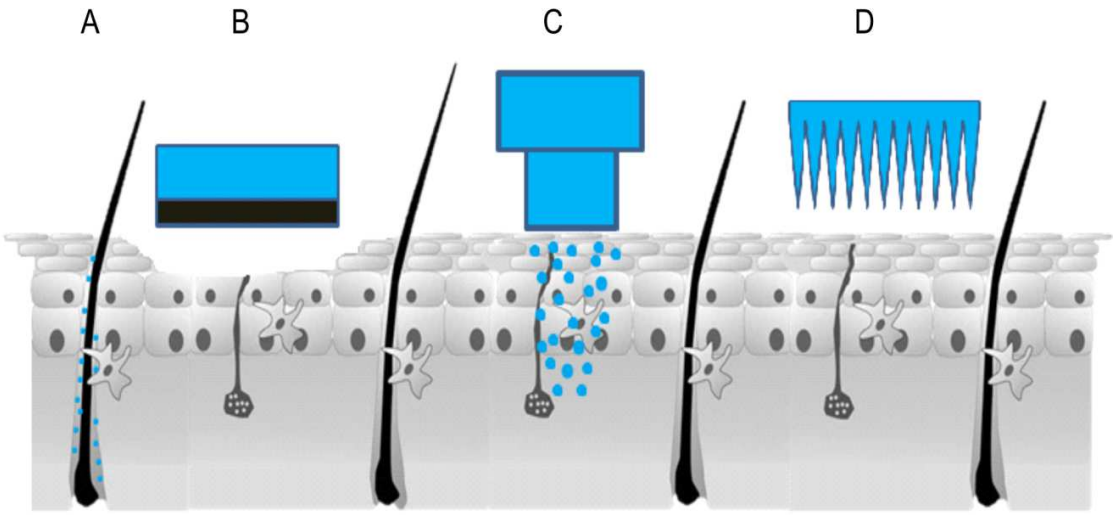

Fig.1: Schematic representation of methods to enable or facilitate TCI: a) transfollicular delivery, b) mechanical dermabrasion, c) jet injection of liquids or powders, d) microneedles (Images are not drawn to scale)

1.5 FACILITATED ABSORPTION METHODS

Particle based vaccines benefit from any form of skin pre-treatment which reduces or removes the SC or any mechanical or electrical application method which transfers them into the epidermis by force (for review see also [20]). Occlusion or chemical penetration enhancers, while enhancing permeation of molecules by several folds due to influencing molecular partition and/or diffusion coefficients, have very little effect on the permeability of particles. [21] Apart from facilitating invasion the barrier disruption additionally causes a non-specific immunostimulation. [22] Often these facilitating methods require special devices. Important points to consider in this context include (i) cost for devices, (ii) ease and

reproducibility of use also by non-trained personnel (e.g. in a pandemic or for mass vaccination in developmental countries lacking medical infrastructure), (iii) severity and area of barrier disruption, time scale of barrier recovery which are connected to the risk of invasion of pathogens through the superficial wound. The severity of these issues varies depending on the type of vaccination which is aspired. Naturally the tendency to tolerate risk is higher with therapeutic vaccines than with prophylactic immunizations.

For example mechanical abrasion of the SC across a large area may be acceptable to improve the permeability of an HIV vaccine. In the DermaVir patch plasmid DNA encoding for 15 HIV antigens is complexed with mannosylated positively charged polyethylene imine to form particles with sizes of 80-400 nm. [23] Mannosylation in this case facilitates the uptake of the particles by APCs. The patch is applied onto skin sites (2-8 areas 80 cm^2 each on the back and the thighs) which are previously being abraded with a DermaPrep medical sponge (Figure 1b). [24, 25] In phase II clinical trials the patch was applied to HIV infected individuals on combination antiretroviral therapy (cART). [24, 25] The treatment was well tolerated also in a dose escalation study; mostly side effects were limited to mild local irritation. [24, 25] The vaccination increased CD-8+ cell counts and may enable intermission of cART. [24]

Devices such as jet-injectors (Figure 1c) or gene guns may relatively easily be compatible with particle based vaccine formulations. The principle relies on the generation of a jet of liquid or powder formulation which is propelled into the skin with great force. Dry formulations have considerable stability advantages. Depending on volume and injection depth a small amount of pain or bleeding and a relatively strong local inflammation may occur. [26] Immunogenicity is reported to be higher or equal to classic vaccine application. [26, 27] The history of using jet-injectors for vaccination goes back to the 1950s. [28] Problems with cases of hepatitis B which were transmitted person-to-person by multi-dose

injectors were overcome by next generation devices which may either be prefilled for single use or come with exchangeable cartridges. [29]

As a third technology with great potential to facilitate the absorption of NPs microneedles (Figure 1d), either solid, hollow, or biodegradable, should be mentioned. They can be used for pretreatment (e.g. Derma Roller) or as a leave on patch which also delivers the formulation. Although not needle-free they reduce sharps associated issues. In contrast to intradermal injections (including the prefilled syringe system BD soluvia which is approved in Europe for influenza vaccination) microneedles only reach the epidermis, stay above the dermal nerve endings and avoid pain. The particles can indeed be integrated in the microneedle arrays. DeMuth et al. constructed a system made from biodegradable antigen loaded MPs. [30] MPs made of poly(lactide-co-glycolide) (PLGA) were embedded in water soluble poly(acrylic acid) (PAA) which actually forms the microneedles. [30] Upon insertion into the skin, PAA dissolves; the microneedles themselves disintegrate and leave a depot of MPs providing controlled release of the antigen. [30] This design may enable separate delivery of a fast (from the matrix) and a slowly available dose (from the MPs, in mice MP-associated fluorescence was demonstrated up to 10 days after microneedle insertion at the site of injection). [30] Likewise the system could be advanced to deliver initial and booster doses of the vaccine in a single application.

1.6 INTRINSIC ADJUVANT EFFECT - INFLUENCE OF PARTICLE PROPERTIES

While for most applications NPs should be inert, that means that complement activation is not desirable, an immuno-stimulatory effect of the nano-formulation may be a benefit for vaccination purposes. Various properties such as size, surface charge and material properties play a vital role in shaping an immune response. A wide variety of particulate systems, including liposomes, virosomes, nanocomplexes

and polymer based carriers are being investigated, all showing a different immunological outcome. For example, a particle based vaccine formulation may be capable of provoking a strong humoral response but fail to generate cellular responses. This might be due to different particle properties.

It is widely accepted that particle based vaccine delivery systems are more immunogenic than soluble antigen as particulate system mimic the size and structure of a pathogen. Among others this is due to the enhanced uptake by APCs. Carrier size also plays an important role in determining the type of response induced. [31] Recently, Mottram et al. showed that small differences in particle size (20-200 nm) influence the cytokine balance after a single immunization, showing that particle size in the range of 40-49 nm induces type 1 (cellular) responses and larger particles with 93-123 nm inducing type 2 (humoral) responses. [32] These findings are especially noteworthy while considering strategies of immunization against viruses where cellular responses are required.

Surface charge of the particles is another vital property which not only determines the stability of particles but plays an important role in contributing the immuno-regulatory effect of the particulate systems. With respect to TCI, Rancan et al. showed that positively charged particulate systems seem to be taken up better by LCs due to electrostatic interactions with cell membrane eventually favouring their internalization. [33] Moreover, Ma et al. showed even the appropriate surface charge density is crucial to have an effective and efficacious immune-regulatory effect. [34]

Finally, particle material may influence immunogenicity. The main function of a material is to stabilize the antigen by protecting it from the surrounding biological conditions, to slow down the clearance of antigens and to enhance delivery to APCs with design constraints such as biodegradability and biocompatibility. One strategy is to use materials extracted from microbial (e.g. total polar lipid extract from archae bacteria, or poly-γ-glutamic acid [35, 36]) to formulate particulate carriers. Interestingly, the materials themselves do not show adjuvant properties when delivered as solution but when formulated

as particulate carrier they up-regulated cytokine responses and MHC molecules, suggesting that particulate formation is necessary for the interaction between materials and certain surface molecule on APCs. [35, 36]

1.7 COUPLING NP WITH ADJUVANTS

Adjuvants are commonly added to vaccine formulations to enhance immunogenicity of poorly immunogenic antigens such as subunit vaccines or to shape the type of immune response, e.g. to increase cellular responses. For the same reasons particulate vaccine formulations may be combined with adjuvants. A variety of adjuvants are being used in clinical testing, marketed formulations as well as in research settings with different mode of actions. An important consideration is the risk of side effects by adjuvants. This is especially true for prophylactic vaccines which are given to healthy people and therefore have to fulfill the strongest safety criteria. For example cholera toxin and E. coli heat labile toxine (LT) are both very effective adjuvants for TCI and are very effective in humans. [37] Nonetheless considering the application of LT as patch against travellers' diarrhea even the appearance of skin rashes and discoloration at the patch site may lead to the termination in a late clinical phase. At present, the choice of adjuvant is a compromise between necessity for adjuvanticity and minimal level of side effects. [38] Nevertheless, combination of adjuvant, antigen and particulate carrier may reduce the dose of antigen as well as adjuvant required in the formulation and consequently minimize the risk of side effects of novel adjuvant candidates for prophylactic vaccines. [39, 40] Adjuvants may either be (i) simply co-administered with encapsulated antigen, (ii) encapsulated in separate particles or (iii) co-encapsulated with the antigen in the same particle. Alternatively the particle surface may be decorated with the adjuvant by physical or chemical association (Fig.2.).

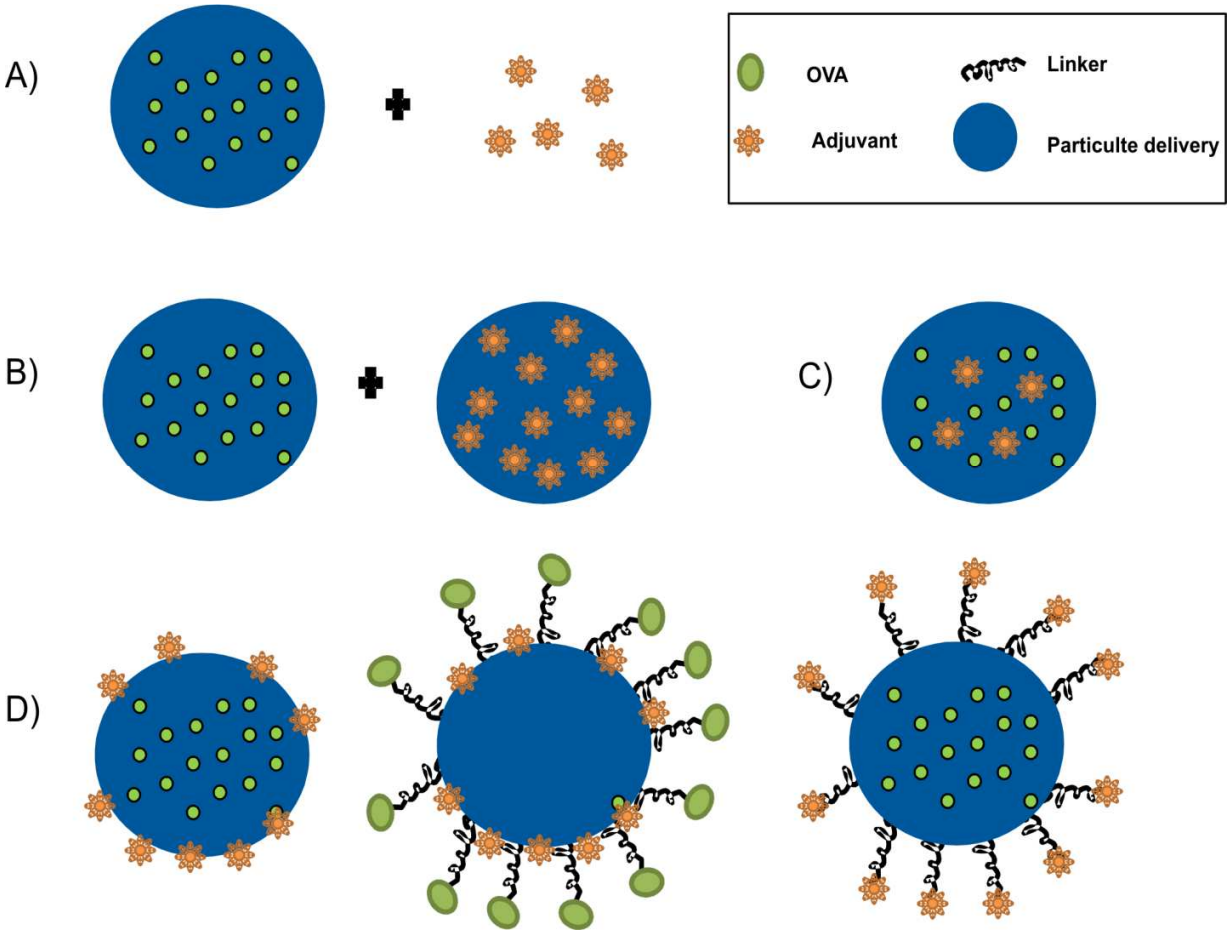

Fig.2: Combinations of antigen and adjuvant in a particulate carrier: a) adjuvants are co-administered with the encapsulated antigen, b) antigen and adjuvant are encapsulated in separate particles, c) antigen and adjuvant are co-encapsulated in same particle, d) the particle surface is decorated with the antigen and/or the adjuvant by physical or chemical association.

Recently, Bershteyn et al. showed that co-delivery of antigen with an adjuvant decorated on the surface of a particle generates humoral as well as cellular immune responses at ultra-low doses (at nanogram levels) of antigen and adjuvant. [41] In the same study, the authors have shown that co-loading of antigen and adjuvant in the same particle after a single immunization was significantly advantageous

compared to antigen and adjuvant delivered on separate particles. But this advantage was lost after a boost immunization, suggesting that after boosting it does no longer matter whether antigen and adjuvant were on the same or separate particles. However, conflicting results exist in literature, whether it is beneficial to co-encapsulate adjuvant and antigen in the same particles or admix the adjuvant just prior to immunization (either in solution or separately encapsulated) in order to generate long lasting immune responses. [42, 43]

Future studies also need to clarify which type of association between adjuvant and particle should be preferred. Conceivably this may depend on the type of adjuvant used. For example, an adjuvant which has receptors expressed on the surface of APCs (e.g. some sugars such as mannose) will probably benefit from being displayed on the particle surface. In contrast, encapsulation of intracellularly processed adjuvants will possibly generate a more robust immune response due to enhanced uptake by APCs and intracellular delivery compared to administration as solution. [44] Overall, combining adjuvant and antigen in particulate carriers either by (co-)encapsulation or admixing is an attractive approach to improve the efficacy of vaccines and reduce the cost of vaccination.

1.8 Conclusion

Altogether particle based vaccines hold great promise for TCI. However, their successful delivery is not without challenge. A product which makes it to the market probably needs to combine particles, antigen, adjuvant, and a device to achieve both a sufficient immunogenicity and sufficient permeation. This naturally increases the regulatory hurdles. At the same time production costs of the product should still be low to extend its affordability beyond the industrialized world. Some of the solutions presented in this overview raise hopes that this may indeed be achievable in the future.

2. AIM OF THE THESIS

The aim of the thesis was to establish in vitro skin models and methods to investigate the uptake of nanoparticles into hair follicles, especially quantitatively to estimate the potential of this type of carriers for transfollicular vaccination.

The following strategy has been used to achieve this objective:

1. Development of a method to quantify the uptake of nanoparticles into hair follicles
2. Verification of the pig ear skin model for quantitative evaluation of nanoparticle uptake into hair follicles in comparison with the situation in vivo in humans
3. Determination of the influence of nanoparticle material on follicular penetration
4. Determination of the influence of application techniques on the extent of nanoparticle penetration into hair follicles
5. Proof of concept studies to evaluate if antigen loaded nanoparticles can induce an immune response via the transfollicular route when applied onto the intact skin barrier

Based on the differential stripping technique a fully quantitative method was developed to monitor the fate of particles applied onto the skin surface (Chapter 3).

The suitability of the pig ear skin model as substitute for human forearm as potential application site was verified in a comparative in vitro-in vivo study (Chapter 3).

The influence of nanoparticle material on hair follicular uptake was investigated with nanoparticles based on PLGA carrying different surface modifications with varying charge and lipophilicity in pig ear as well as in human volunteers (Chapter 3).

As the amount of deliverable drug is very limited, methods to enhance the uptake of nanoparticles into hair follicles are highly relevant. A well-known phenomenon in hair follicle targeting described in the literature is the penetration depth enhancing effect of massage. To clarify if this effect is not only qualitative but also quantitative, the uptake of fluorescently labeled PLGA nanoparticles applied with and without massage was investigated (Chapter 4).

Moreover nanoparticle-based formulations are known to penetrate the hair follicle deeper than liquid formulations. The extent of the superiority of nanoparticles compared to solutions was determined as well (Chapter 5).

For prove of concept transfollicular vaccination across the intact skin was investigated using OVA loaded PLGA and Chit.-PLGA nanoparticles. Stability, biological activity and immunogenicity of the model antigen OVA were assessed. An adoptive transfer model in mice should clarify if a successful antigen delivery and immunization via the transfollicular route without pretreatment of the skin is possible.

The thesis will be organized in three chapters entitled:

Chapter 3: “Quantification of nanoparticle uptake into hair follicles in pig ear and human forearm”

Chapter 4: “Influence of application technique on the uptake of nanoparticles into the hair follicle”

Chapter 5: “Non-invasive delivery of nanoparticles to hair follicles – a perspective for transcutaneous immunization”

3. QUANTIFICATION OF NANOPARTICLE UPTAKE INTO HAIR FOLLICLES IN PIG EAR AND HUMAN FOREARM

Parts of this chapter have been published as:

A. S. Raber, A. Mittal, J. Schäfer, U. Bakowsky, J. Reichrath, T. Vogt, U. F. Schaefer, S. Hansen and C.-M. Lehr, Quantification of nanoparticle uptake into the hair follicles in pig ear and human forearm, Journal of controlled release 179 (2014) 25 - 32

The author of the thesis made the following contributions to the publication:

Planned, performed and interpreted all major experiments, wrote the manuscript.

3.1 INTRODUCTION

Recently hair follicles (HF) gained attention as an alternative pathway for dermal absorption which often facilitates permeation. Despite a relatively low surface coverage of ca. 0.1% [45] the HF contribute significantly to the absorption of small molecules, especially those with low to intermediate octanol-water partition coefficients [46], and importantly, also to the absorption of (sub)micron particles [11]. In fact, for drug delivery approaches the HF represent interesting target sites. Due to the slow clearance rate by sebum flow and hair growth especially NP build a depot inside the HF where they are protected from contact with clothing and are not easily washed off [47]. Also, the SC is absent in the lower third of the HF which facilitates the absorption of substances. Thus transfollicular delivery has been investigated in the context of needle free vaccination [48], delivery strategies for macromolecules [49, 50], NP-based sunscreens [51], as well as for risk assessment applications [52]. Moreover, for HF related disorders such as alopecia [53, 54] or acne [55], the HF itself is the target site.

To improve therapeutic drug delivery via the HF it is of interest to optimize NP in a way that achieves the highest possible uptake into the HF. It is well established that NP invade deeper into HF than solutions [56] and that invasion depth depends on particle size. From cross-sections of terminal HF on pig ear an optimum particle size of ca. 645 nm was identified, which seems to be independent of particle composition [11]. Therefore a mechanical effect for follicular entry has been postulated [11]. Besides the penetration depth, the amount of NP delivered into the HF is of interest as it allows for example comparing the efficacy of therapeutic treatments by comparing the delivered dose of an encapsulated active and optimizing the targeting efficiency of NP into the HF. The differential stripping technique should be suitable to quantify follicular uptake. This technique relies on first sampling the SC by tape stripping to evaluate the portion of analyte deposited on the skin surface and penetrated into the SC and

separately sampling the HF content by a cyanoacrylate (superglue) biopsy. Differential stripping has been applied before in vitro on the pig ear model as well as in human volunteers to qualitatively and semi-quantitatively investigate follicular uptake of fluorescent solutions as well as a number of model NP or sunscreens [57, 58]. This was done by relating the amount of fluorescent NP recovered from the HF to the amount remaining on the skin surface. However, by demonstrating mass balance and coupling differential stripping with a sufficiently sensitive and robust analytical method (e.g. fluorescence spectrometry, HPLC-UV/MS, scintillation counting depending on NP cargo or label) it should be possible also to use the method for quantifying NP distribution after topical application, and particularly for quantifying NP uptake into HF.

There are only two studies investigating the influence of particle size, surface charge, material and shape on the uptake across the inter-follicular epidermis. However, follicular targeting was not addressed in particular. Labouta et al. found greater skin penetration of gold NP with a hydrophobic surface [59]. Lee et al. found negatively charged gold nano rods to be superior compared to positively charged nano rods [60]. It is currently not known whether these results are also relevant to uptake into the HF. Furthermore it has been shown before that the penetration of superfine particles is quite different from NP a few 100 nm in size or MP [61]. It is therefore uncertain whether the results for superfine particles can be extended to larger particles. In this study we developed a method to quantify NP uptake into HF and applied it in vitro in a pig ear model and in vivo in human volunteers. This method allows investigating the uptake of NP into HF systematically. The HF is filled with sebum, and therefore provides a mainly lipophilic environment [62]. Therefore we hypothesized that lipid coating may facilitate NP uptake into HF. To exclude size effects we used NP of similar hydrodynamic sizes (163-170 nm) but different surface modifications. As it is known that phospholipids (PL) are part of the sebum we investigated systematically quantitative HF deposition with fluorescence labeled NP based on PLGA: i) plain PLGA; ii)

chitosan coated PLGA (Chit.-PLGA); and iii) Chit.-PLGA coated with different phospholipids (PL) DPPC (100), (DPPC : Chol (85 : 15), DPPC : DOTAP (92 : 8). Differential stripping was performed including complete mass balance. The samples were extracted for fluorescence quantification. An effect of the PL coating on follicular uptake was observed as plain DPPC and DPPC : DOTAP (92 : 8) penetrated into HF to a higher extent than the other tested NP. The effect was observed both in vitro in a pig ear skin model as well as in vivo in human volunteers, although it was statistically significant only in the in vitro model. An excellent in vitro in vivo correlation (IVIVC, $r^2 = 0.987$) between both models was demonstrated, further supporting the suitability of the pig ear model as a surrogate for the in vivo situation in humans to study NP uptake into HF quantitatively.

3.2 Experimental Methods

3.2.1 Chemicals and Methods

We purchased PLGA (Resomer RG 50:50 H; inherent viscosity 0.31 dl/g) from Boehringer Ingelheim GmbH & Co. KG, Ingelheim, Germany; ultrapure chitosan chloride salt (Protasan® 8 UP CL113) from FMC BioPolymer AS, Oslo, Norway; polyvinyl alcohol Mowiol® 4-88 (PVA) from Kuraray Specialties Europe GmbH, Frankfurt, Germany; Tesa film from TESA SE, Hamburg, Germany; and nano screen-MAG NP from chemicell GmbH, Berlin, Germany. All other solvents and chemicals used were of the highest purity available. Deionized water (dd water, Milli Q Plus system, Millipore, Bedford, MA, USA) was used throughout.

3.2.2 *PIG EAR SKIN AND HUMAN VOLUNTEERS*

Pig ears were obtained from a local abattoir from freshly slaughtered pigs removed before scalding. Only ears with immaculate skin surface were used. Ears were stored at 2 – 8 °C for a maximum of two days. Treatment occurred on the outer auricle.

Eleven volunteers (Caucasian, five female, six male, skin type II – IV) with no history of skin disease participated in the study, which was approved by the "Ärztekammer des Saarlandes" ethical committee and in adherence with the Declaration of Helsinki Principles. All volunteers signed informed consent. Treatment occurred on the outer forearm due to the larger number of hair follicles compared to the inner forearm. Subjects were asked not to use any cosmetics on the application site on the day of the experiment.

3.2.3 *NANOPARTICLES*

For visualization nano screen-MAG nanoparticles (chemicell GmbH, Berlin, Germany) were used. The particles have a hydrodynamic diameter of 100 nm and are fluorescently labeled. They are composed of a solid magnetite core and covered with a chitosan matrix. The nano screen-MAG serve as model NP as they are visible on the skin by eye due to their dark brown color as well as by fluorescence and environmental scanning electron microscopy ESEM microscopy.

PLGA-NP were prepared by a double emulsion method described in [48]. Chit.-PLGA NP were prepared by the emulsion-diffusion-evaporation technique described in [63]. For PL coating Chit.-PLGA NP were incubated with large, unilamellar vesicles consisting of DPPC, a mixture of DPPC : Cholesterol (85:15), or DPPC : DOTAP (92:8) respectively. Via ultrasonification the lipids formed self-organized PL bilayers on the NP surface [63]. PLGA was covalently labeled with fluoresceinamine (FITC-PLGA) according to [64] to

prevent the label from leaking from the NP and avoid free dye diffusion. Cleavage of FITC-PLGA by esterases in the skin is not relevant within the timeframe of the experiment [64].

PLGA NP were stored as freeze-dried powder and re-suspended in dd water to obtain the desired concentration prior to use. Chit.-PLGA NP and PL coated Chit.-PLGA NP were stored as stable suspension at 4-8° C for a maximum of 14 days after manufacturing. Immediately before each experiment the hydrodynamic diameter, size distribution, and zeta potential were determined using a Zetasizer Nano-ZS (Malvern, Malvern UK).

3.2.4 APPLICATION PROTOCOL AND SAMPLING

The same standardized application and sampling protocol was used for pig ears in vitro and human volunteers. The ears and outer forearm was wiped with cold water, blotted dry with tissue and allowed to dry completely. Hairs were shortened with scissors and incubation sites of 1.767 cm^2 were marked with water resistant marker. PLGA NP were tested on 4 ears with 2 application areas each and 6 volunteers with 3 application sites each; plain and PL-coated Chit.-PLGA NP were tested on 3 ears with 2 application sites each and 5 volunteers with 1 application sites each. On each ear and in each volunteer one additional area received blank formulation (dd water). Due to space limitations not all particles can be tested in the same volunteers. The results are nonetheless comparable between particles due to subtracting blanks obtained for each individual. 15 µl of PLGA NP suspension were applied, and massaged for three minutes with a gloved forefinger. Due to constraints from manufacturing the concentration of plain and PL coated Chit.-PLGA NP was much lower than for PLGA NP. In order to obtain reasonable quantification limits a higher volume of 30 µl of NP suspension was applied, and no massage was performed to avoid removal of formulation. Instead the suspension was carefully distributed with a pipette tip. The formulation remained on the skin of the volunteers for one hour without coverage. Pig

ears were kept in an incubator at 32° C for an equal time period. The temperature of 32° C is equivalent to the human skin surface temperature and is recommended for the performance of in vitro skin experiments [65]. Afterwards the skin distribution of the NP was analyzed by extracting the following sample fractions:

(a) 10 Tape strips were taken to collect NP remaining on the skin surface. To standardize the pressure with which each tape was pressed onto the skin surface and to minimize the influence of furrows and wrinkles a roller device was used [66]. The first and second tape strips were extracted separately. Subsequent tape strips were extracted in pairs of two. (b) Two cyanoacrylate biopsies were performed putting a drop of superglue in the center of the incubation site and covering it under slight pressure with a tape strip. The glue was allowed to polymerize completely for at least 5 min and the tape strip was removed with a quick movement containing the cast of the HF including the NP. (c) For mass balance a punch biopsy of 4.91 cm^2 including the incubation site was taken from pig ear skin to sample the skin rest. In the volunteers the same area was swabbed with cotton soaked in ethanol instead. The solvent was allowed to evaporate completely before extraction. (d) Also the application devices (glove fingers for PLGA NP, pipette tip for PL-coated Chit.-PLGA NP) were extracted.

3.2.5 SAMPLE EXTRACTION AND QUANTITATIVE ANALYSIS

All samples were extracted in acetonitrile (ACN) : 0.1 N sodium hydroxide (NaOH) (70:30) for three hours under light exclusion and then centrifuged (5 min, 20 °C, 24651 g). Fluorescence intensities of all samples were measured (excitation λ_{ex} = 490 nm, emission λ_{em} = 525 nm) in a plate-reader (TECAN infinite M200, Tecan GmbH, Crailsheim, Germany). For calibration, a stock suspension with known NP concentration (wt/V) was prepared in ACN : 0.1N NaOH (70:30), extracted for three hours and diluted with ACN : 0.1N NaOH to obtain standards.

3.2.6 *NP VISUALIZATION ON SKIN*

15 µl nano screen-MAG NP suspension (0.375 mg NP) were applied onto pig ears. Incubation and sampling was performed as described above. Scan images of the incubation sites were taken using a flatbed scanner (Epson Perfection 3200 Photo, 600 dpi, 24 Bit) (i) of the incubated area, (ii) after performing ten tape strips, and (iii) of a non-incubated reference area. Furthermore, cyanoacrylate biopsies were investigated by light microscopy (Olympus BH 2, 20-fold magnification).

Additionally, the tape strips, skin sample after tape stripping and cyanoacrylate biopsies were visualized by confocal microscopy (LSM 510 Meta, Carl Zeiss GmbH, Jena Germany). Auto fluorescence of the skin samples, tapes and cyanoacrylate was compensated by using λ_{ex} = 458 nm and band pass filter 520-555 nm. The microscopic settings were adjusted using tape strips and cyanoacrylate biopsies from a blank experiment as negative and a droplet of NP-suspension distributed on an objective slide as positive control.

The same kind of skin samples were further imaged by environmental scanning electron microscopy (ESEM, Quanta 400 FEG, FEI Deutschland GmbH, Germany) in low vacuum mode at a pressure of 100 Pa and an acceleration voltage of E = 20 keV. A large field detector was used to image topography. A solid state detector was used to enhance contrast between skin, hairs and the metal core NP. Three regions of interest (ROI) were determined on the hair, the skin surface and near the HF orifice and x-ray spectra were obtained using an EDAX Genesis V 6.04 analysis system at E = 20 keV

3.2.7 *METHOD VALIDATION*

Lower limits of detection (LLOD) and of quantification (LLOQ) of (i) all tape strips, (ii) cyanoacrylate biopsies, (iii) both application devices (glove finger, pipette tip), (iv) cotton swab, and (v) skin rest were

calculated by averaging the fluorescence intensity obtained from blank experiments by applying dd water instead of NPs (in vitro: n=23, in vivo: n=11). Extreme outliers of all blank values were removed separately for each group (i) to (v) by applying the following protocol: Initially, the first quartile Q_1 (25^{th} percentile), third quartile Q_3 (75^{th} percentile) and interquartile range (IQR, difference between Q_3 and Q_1) were calculated. Subsequently, all data points outside the [Q1 - 3×IQR, Q3 + 3×IQR] interval were removed from the data sets. LLOD and LLOQ were defined as the mean fluorescence intensity plus twice or thrice the standard deviation of the adjusted data sets, respectively. The intra- and inter-ear variability was determined from blank experiments on 4 ears with 3 application sites each. For the cyanoacrylate biopsy, the application device, and the skin rest the intra-ear variability was calculated from the relative standard deviation (%SD) between all samples obtained from the same ear. The inter-ear variability was calculated from relative SD between all samples obtained from all 4 ears.

3.2.8 STATISTICS

Statistical testing was performed by one-way ANOVA with Holm-Sidak all pairwise multiple comparison procedure.

3.3 RESULTS AND DISCUSSION

3.3.1 NP CHARACTERIZATION

The properties of the investigated NP are summarized in table 1. All NP have different compositions and were prepared by two different preparation techniques. Non-modified PLGA particles were prepared by a double emulsion method with PVA as stabilizer. Plain and PL coated chitosan modified PLGA NP were prepared by an emulsion-diffusion-evaporation technique. With both

techniques the particle size can be adjusted by using the correct conditions, e.g. stabilizer-concentration or speed of the homogenizer.

PLGA NP have a negative zeta potential, Chit.-PLGA and PL-coated Chit.-PLGA NP have positive zeta potentials of similar magnitude. We consider PL-coated NP to have more lipophilic surface properties than the other two, although there is to date no convenient and reliable method to quantify NP surface lipophilicity [67].

Table 1 Particle characterization. Mean ± SD of n = 3 individually prepared batches

	PLGA NP	**Chit.-PLGA NP**	**DPPC : Chol (85:15) coated Chit.-PLGA NP**	**DPPC : DOTAP (92:8) coated Chit.-PLGA NP**	**DPPC (100) coated Chit.-PLGA NP**
Hydrodynamic size (nm)	162.8 ± 0.06	167.3 ± 3.0	158.9 ± 0.9	156.6 ± 1.8	169.6 ± 3.0
PDI	0.06 ± 0.01	0.16 ± 0.03	0.10 ± 0.02	0.17 ± 0.01	0.23 ± 0.01
Zeta potential (mV)	-33.6 ± 2.5	30.0 ± 3.2	26.6 ± 0.8	27.5 ± 0.9	17.0 ± 1.4

3.3.2 NP VISUALIZATION ON SKIN

It is necessary to show that differential stripping is able to separately sample the NP from the skin surface including wrinkles and dermatoglyphs and the HF. Due to the size of the NP used in this study and their rigidity one can exclude that they enter the intact SC of human or pig skin [61].

Figures 1a and 1d show scan and ESEM images of 100 nm fluorescently labeled nano screen-MAG on the skin surface of a pig ear in comparison to the surrounding non-incubated area. Nano screen-MAG were homogenously distributed across the incubation site (Fig.1 a). After ten tape strips the brown color

remained only in the orifices of the HF (Fig.1 b+e) which could be removed by two cyanoacrylate biopsies (Fig.1 c+f). In agreement with that, fluorescence microscopy showed decreasing nano screen-MAG fluorescence intensity from tape 1 to 7, while no fluorescence was present on tape 8 to 10 and on the surface of tape striped skin (Fig.2a). The fluorescence intensity (excitation wavelength 476 nm, emission wavelength 490 nm) quantified after extracting the tapes decreased steadily from tape 1 to 10, with less than 1.5% of the total applied amount being found in the last two tape strips (Fig. 2b). Three different regions of interest were defined (ROI): (ROI 1) an area supposedly being covered with NP, (ROI 2) the hair, and (ROI 3) the skin surface (Fig. 3a). Spectral analysis revealed the molecules typical of the respective areas, i.e. (ROI 1) iron indicating the magnetite core of nano screen-MAG, (ROI 2) carbon and sulfur indicating the hair disulfide bonds of hair keratin, and (ROI 3) carbon indicating the skin surface (Fig. 3b). In summary these analyses confirmed the efficacy of surface cleaning by ten tape strips and gave convincing evidence that the fluorescence recovered from cyanoacrylate biopsies is representative of the HF content.

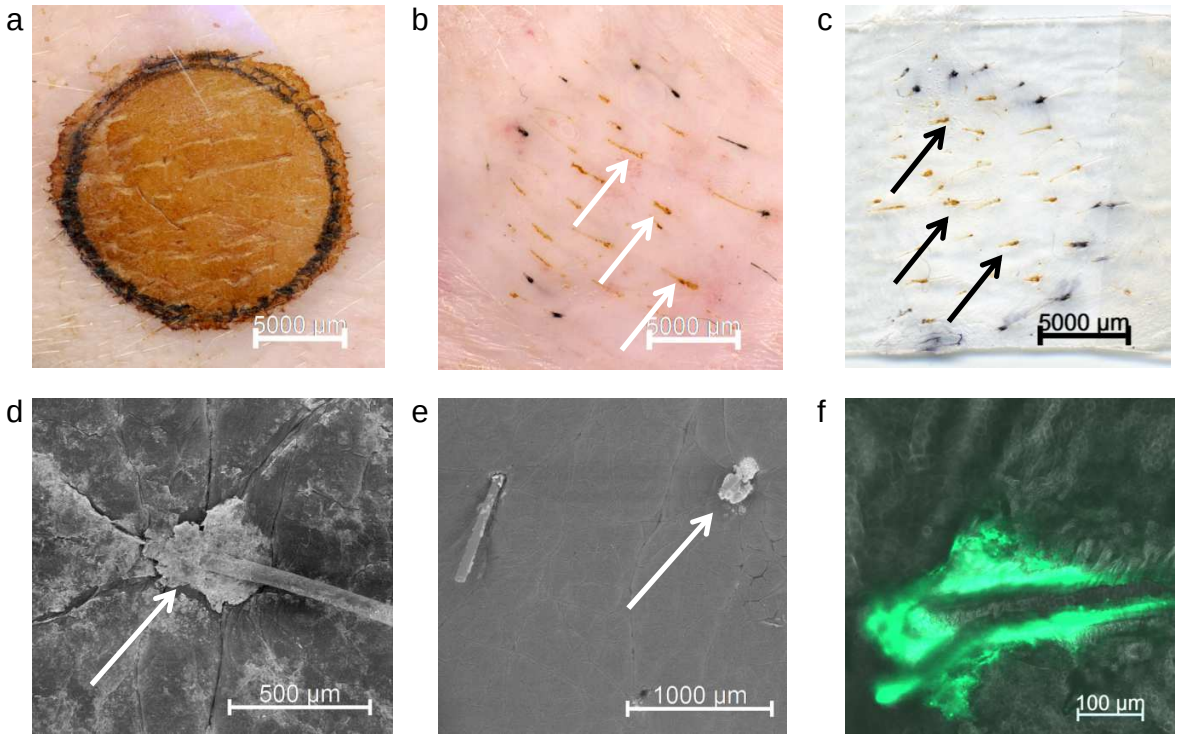

Fig. 1: Skin distribution of nano screen-MAG NPs (100 nm, magnetite core, chitosan coated, fluorescence labeled, λ_{ex} 476 nm, λ_{em} 490 nm) investigated on pig ear skin. a-c: Scan images (scale bar = 5 mm); d, e: ESEM images, f: Confocal microscopy of a cyanoacrylate biopsy, a focal plane of a representative HF (scale bar = 100 µm); a+d: NPs are distributed homogeneously across the incubation site; b+e: After application of ten tape strips no NPs remain on the skin surface. NPs deposited in the HFs are clearly visible; c+f: A cyanoacrylate biopsy performed after tape stripping. The content of the HF is incorporated in the polymerized cyanoacrylate, NPs are clearly visible.

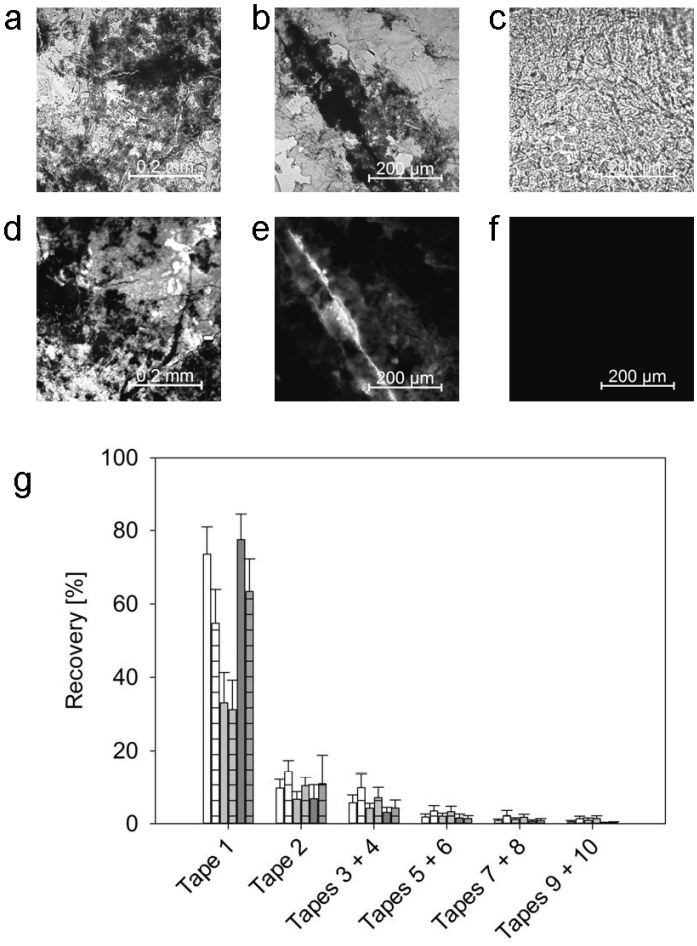

Fig. 2: Pig ears were incubated with nano screen-MAG NP and differential stripping was performed as described. (a-c) Transmission images showing stratum corneum removed by tape stripping and (d-f) showing fluorescence from nano screen-MAG NP (λ_{ex} = 458 nm, band pass filter 520-555 nm LSM 510 Meta, Carl Zeiss GmbH, Jena Germany). Nano screen-MAG NP are visible on tape strip #1 (a, d) and #2 (b, e), but no longer on tape strip #10 (c, f).

(g) Skin was incubated with FITC labeled PLGA NPs (light grey bars), Chit.-PLGA NPs (dark grey bars) and DPPC-Chit.-PLGA-NPs (white bars) and differential stripping was performed as described (In vitro: pig ear skin (plain bars), in vivo: human forearm (striped bars)). The samples were extracted and fluorescence intensity was quantified to calculate %recovery. Less than 1.5% of the total applied amount of any NP was found in tapes 9+10.

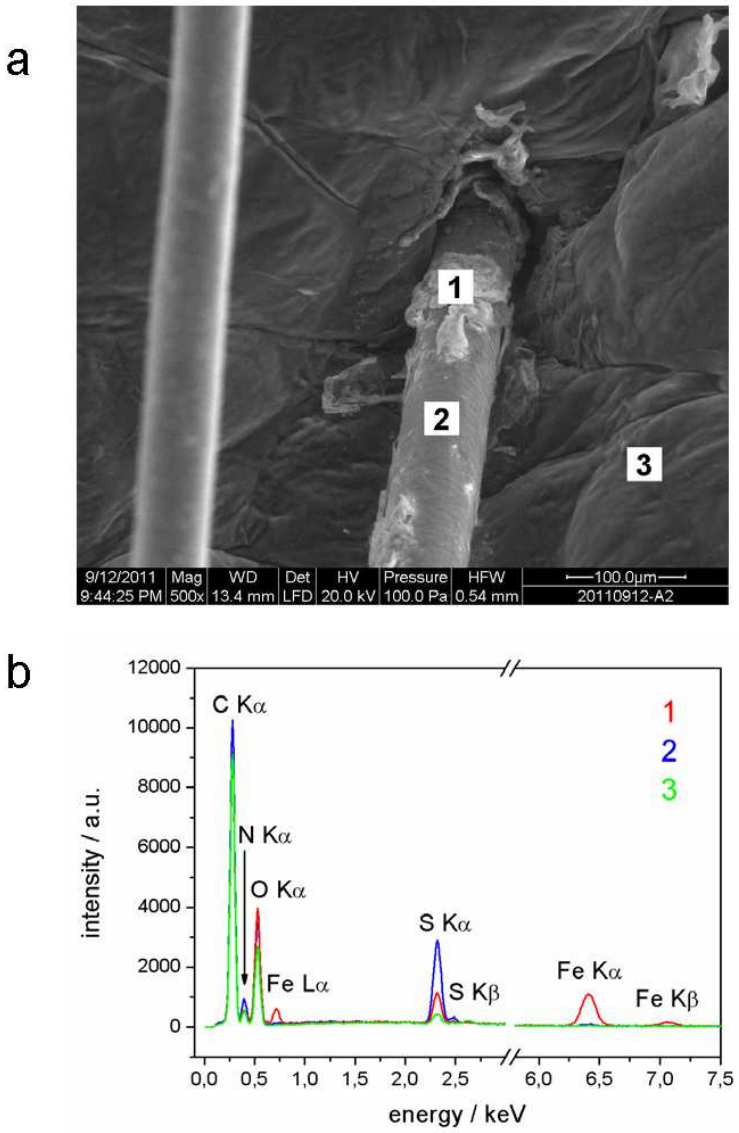

Fig. 3: (a) ESEM image of pig ear skin incubated with nano screen-MAG NPs after performing ten tape strips. ROIs were defined on areas supposedly containing NPs (ROI 1), the hair (ROI 2) and on the skin surface (ROI 3) and spectral analysis was performed (b). Iron from the nano screen MAG NP core was detected only in ROI 1.

3.3.3 METHOD VALIDATION

LLOQ were similar for pig ear and human skin which is important for IVIVC. The intra-ear variability for cyanoacrylate biopsy, application device, and skin rest was smaller than the inter-ear variability. Only for tape strips intra- and inter-ear variability were similar. Consequently, for each ear a new blank experiment needs to be performed, however it is sufficient to perform just one blank experiment per ear.

The brightness of the NP fluorescence and the background fluorescence of the matrix determine the LLOQ and therefore represent the analytical constraints of the quantification method.

Table 2 summarizes linear range of particle fluorescence in ACN : 0.1 N NaOH 70:30 and LLOQ. Due to the different types of matrix LLOQ is different for tape strips, cyanoacrylate biopsies, skin rest (in vitro)/ cotton swab (in vivo), and application devices (glove finger, pipette tip). LLOQ was calculated for each type of matrix from mean fluorescence intensities obtained from blank experiments applying water instead of NP plus three times the standard deviation. For tape strips, cyanoacrylate biopsies, application device, and the skin rest 17 out of 138, 2 out of 46, 3 out of 14, and 2 out of 23 (in vitro) and 4 out of 66, 3 out of 22, 1 out of 6, and 0 out of 11 (in vivo) were discarded as outliers, respectively. The highest LLOQ was measured in cyanoacrylate biopsies which are therefore the limiting factor of this quantification method (Table 2).

For example, LLOQ should not be higher than 3.75-7.5 µg/ml to be able to quantify 1-2% of the applied amount in each matrix type (assuming that 15 µl of a 50 mg/ml NP dispersion are applied onto the skin). This was the case for all NP and matrices in vitro as well as in vivo. LLOQ were similar for pig ear and human skin which is important for IVIVC.

The intra-ear variability for cyanoacrylate biopsy, application device, and skin rest was smaller than the inter-ear variability. Only for tape strips intra- and inter-ear variability were similar (data not shown). Consequently, for each ear a new blank experiment needs to be performed, however it is sufficient to perform just one blank experiment per ear.

Table 2 Linear range of particle fluorescence and LLOQ are reported as NPs concentration in ACN: 0.1 N NaOH, 70:30, [µg/ml]. LLOQ was calculated for each type of matrix from mean fluorescence intensities obtained from blank experiments applying water instead of NP plus three times the standard deviation (n=23 and 11 for pig ear skin and human skin, respectively).

	PLGA		**Chit.-PLGA**		**DPPC-Chit.-PLGA**	
Linear range [µg/ml]	1-375 (r^2>0.999)		0.07-26 (r^2=0.999)		0.07-26 (r^2=0.999)	
LLOQ [µg/ml]	**in vitro**	**in vivo**	**in vitro**	**in vivo**	**in vitro**	**in vivo**
Tape strips	0.18	0.23	0.03	0.03	0.04	0.04
Cyanoacrylate biopsies	3.83	4.12	0.54	0.58	0.75	0.81
Skin rest/cotton swab	1.90	0.55	0.27	0.08	0.37	0.11
Application device	0.17	0.33	0.02	0.05	0.03	0.06

3.3.4 NP UPTAKE INTO HAIR FOLLICLES IN VITRO AND IN VIVO

Tape stripping is a minimally invasive technique which is regularly applied in human volunteers in vivo, for example as a method for determining bioavailability of topically applied formulations [68]. We monitored by measuring transepidermal waterloss (TEWL) that also differential stripping by adhesive tape and subsequent application of two cyanoacrylate biopsies can be applied in human volunteers and is minimally invasive (Fig. 4). Baseline TEWL (Biox Aquaflux AF 200, Biox Systems Ltd., London, UK) of a

control area of untreated skin remained constant during the whole experiment. After 10 x tape stripping, TEWL increased only slightly above baseline indicating negligible barrier damage (from 14.30 ± 1.21 g/m²/h to 18.69 ± 2.29 g/m²/h; mean ± SD of n = 20 respectively). After two cyanoacrylate biopsies TEWL increased distinctly to 64.70 ± 25.75 (Fig. 4a, mean ± SD of n = 20), and remained high during the following 24 h. Typically TEWL > 60 g/cm²/h indicates significant skin damage due to complete SC removal [69]. A slight inflammation of the treated area is expected and disappears within several days. TEWL was monitored in one volunteer until full recovery of baseline values which was observed after 4 days (Fig. 4b).

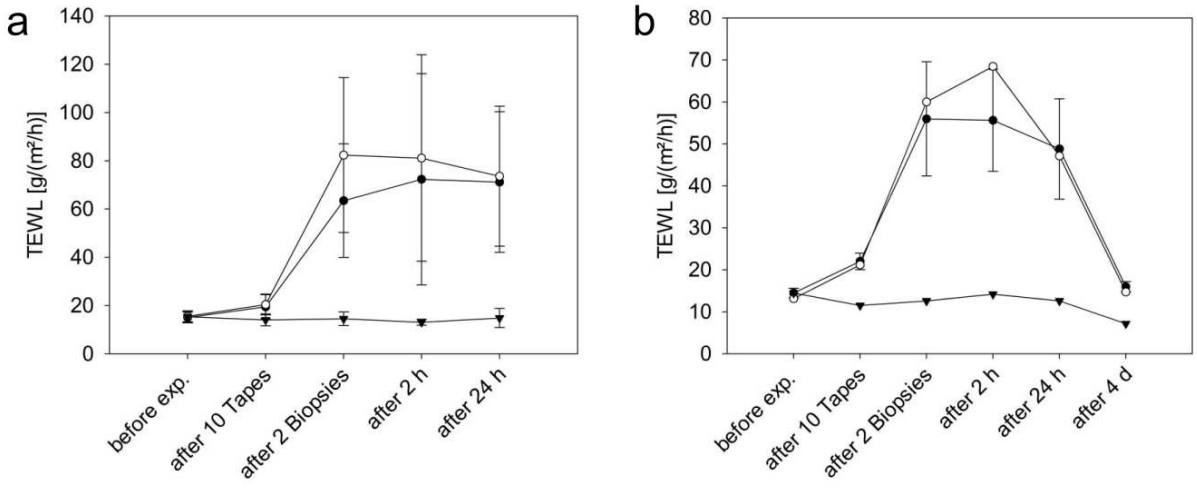

Fig. 4: a: In human volunteers TEWL was measured before the experiment, after 10 x tape stripping, after cyanoacrylate biopsies and again after a recovery time of 2 h and 24 h on one untreated area (baseline, filled triangles), one blank incubation sites (dd water, open circle), and on up to three NP application sites (filled circles). (mean ± SD of n = 10 for blank incubation sites and untreated skin, and n=25 for NPs); b: In one volunteer, additionally TEWL was monitored until full barrier recovery after 4 days, this volunteer received NP on 3 application sites (mean ± SD, filled circles), one blank incubation site (open circles). Base line TEWL was monitored on one untreated skin area (filled triangles).

Table 3 shows the fractions of NP which were recovered from the individual types of samples in vitro obtained from pig ears and in vivo from the forearms of human volunteers. The absolute amount of NP in each sample was determined by fluorescence quantification and related to the total amount of NP applied onto the skin to obtain recovery% (0.424 mg PLGA NP/cm² and 0.059 mg plain or PL coated Chit.-PLGA NP, all representing finite doses). Total recovery% represents the sum of the NP found in all types of samples. OECD (Organisation for Economic Cooperation and Development) test guidelines for skin absorption testing in vitro and in vivo highly recommend mass balance for finite dose studies and define an adequate recovery of 100 ± 10% [70, 71], SCCNFP (Scientific Committee on Cosmetic Products and Non-food Products) accepts 100 ± 15% [72]. Total recovery% usually met the OECD criteria and was always within the SCCNFP limits (Tab. 3).

Table 3 NPs recovered from skin surface, HF, and application device and skin rest (in vitro)/ cotton swab (in vivo) and reported as % (wt/wt) of the total applied dose. Mean ± standard deviation (SD) of n = 8, 17, 6, 5 for PLGA-NPs in vitro, and in vivo and for Chit.-PLGA-NPs and phospholipid coated--Chit.-PLGA-NPs in vitro, and in vivo respectively.

	PLGA NP	**Chit.-PLGA NP**	**DPPC : Chol (85:15) coated Chit.-PLGA NP**	**DPPC : DOTAP (92:8) coated Chit.-PLGA NP**	**DPPC (100) coated Chit.-PLGA NP**
	in vitro				
Skin surface	48.06 ± 8.61	89.79 ± 3.64	86.42 ± 3.36	89.76 ± 5.27	91.71 ± 3.85
HF	**3.61 ± 0.95**	**3.15 ± 1.23**	**2.16 ± 1.11**	**6.04 ± 2.13**	**6.95 ± 2.30**
Skin rest	0.56 ± 0.54	0.05 ± 0.11	0.11 ± 0.09	0.12 ± 0.09	0.25 ± 0.20
Application device	32.26 ± 11.57	5.96 ± 1.93	9.49 ± 4.62	5.28 ± 1.53	9.62 ± 2.85
Total recovery	**84.48 ± 6.82**	**98.96 ± 5.27**	**98.10 ± 4.41**	**101.22 ± 6.09**	**108.53 ± 6.82**
	in vivo				
Skin surface	55.32 ± 8.22	81.02 ± 11.23	84.72 ± 3.99	84.03 ± 5.48	85.26 ± 2.88
HF	**4.82 ± 2.72**	**1.45 ± 0.57**	**1.75 ± 0.75**	**3.80 ± 1.58**	**5.63 ± 3.45**
cotton swab	0.40 ± 0.54	0.01 ± 0.03	0.01 ± 0.03	0.02 ± 0.02	0.06 ± 0.07
Application device	29.37 ± 8.10	7.15 ± 3.07	7.95 ± 3.82	5.86 ± 1.48	6.97 ± 2.26
Total recovery	**89.91 ± 10.14**	**89.63 ± 9.05**	**94.43 ± 5.0**	**96.17 ± 2.52**	**98.10 ± 4.41**

Full mass balance should replace the common praxis in differential stripping studies of reporting relative numbers: usually, the amount recovered from the HF is normalized to a reference value, e.g. by comparing NP versus solutions [73], the same NP formulation over time [47], or worse, the amount recovered from the HF is related to the amount recovered from the skin surface. This HF/surface ratio is in principle an interesting number to demonstrate the relative distribution of NP. However, Teichmann et al. reported a total recovery of only 54±8% for sodium fluorescein solution with the remaining 46% not being accounted for [57]. Problems arise if recovery varies between repetitions, different formulations, or between the different samples obtained (i.e. the recovery is different from tape strips and cyanoacrylate biopsies) as it can seriously distort results. The major advantage of reporting absolute, non-normalized numbers is that the absolute amount of active pharmaceutical ingredient or NP taken up into HF can be determined. This number is relevant to determine the deposited dose.

By quantitative differential stripping analysis we found that, although the major fraction of NP remained on the skin surface (48-55% when NP were applied with a gloved forefinger, 81-92% when NP were applied by pipetting), depending on NP material 1.45-6.95% of the applied NP penetrated into the HF (Tab. 3). The different fractions deposited on the skin surface are clearly linked to the different fractions of NP remaining on the application devices (ca. 30% when NP were applied with a gloved forefinger, ca. 5-10% when NP were applied by pipetting, Tab. 3). Furthermore, both in vitro and in vivo follicular uptake was dependent on NP material. In vitro in pig ears DPPC coated, and DPPC : DOTAP (92 : 8) coated Chit.-PLGA were those NP which were taken up to the highest extent, while plain PLGA, Chit.-PLGA and DPPC : Chol. (85 : 15) coated Chit.-PLGA NP were taken up less efficiently. Differences between both DPPC coated as well as DPPC : DOTAP (92 : 8) coated Chit.-PLGA NP and each of the other NP, i.e. plain PLGA, Chit.-PLGA and DPPC : Chol. (85 : 15) coated Chit.-PLGA NP were significant (Tab. 3, Fig. 35, one-way ANOVA with Holm Sidak all pairwise multiple comparison, $p<0.05$ indicating significance). To

confirm these findings, the experiments were repeated in human volunteers. The outer forearm was chosen as this is more densely covered with follicles than the inner forearm (which usually would be the recommended application site for testing delivery from topical formulations in vivo in humans [70]. The same phenomenon of two groups was found. In vivo the difference between plain PLGA, DPPC coated, and DPPC : DOTAP (92 : 8) coated Chit.-PLGA NP on the one hand and Chit.-PLGA and DPPC - Chol. (85 : 15) coated Chit.-PLGA NP was more obvious (Tab. 3 Fig. 5a). However, due to a higher variability of the in vivo data the differences were not statistically significant (one way ANOVA with Holm Sidak all pairwise multiple comparison, $p<0.05$ indicating significance). To test the hypothesis that the pig ear is a suitable model for the situation in man for quantifying follicular uptake of NP, we correlated in vitro with in vivo results by plotting mean ± SD of % recovery from all sample fractions (except skin rest and cotton swab as different methods were applied in vitro and in vivo) and found an excellent linear IVIVC ($r^2=0.987$, Fig. 4b). Additionally we correlated the in vitro versus in vivo mean recovery% only from the HF and still obtained a distinct relationship which is however not as clear due to the high variability of the individual data points ($r^2=0.577$, Fig. 5c).

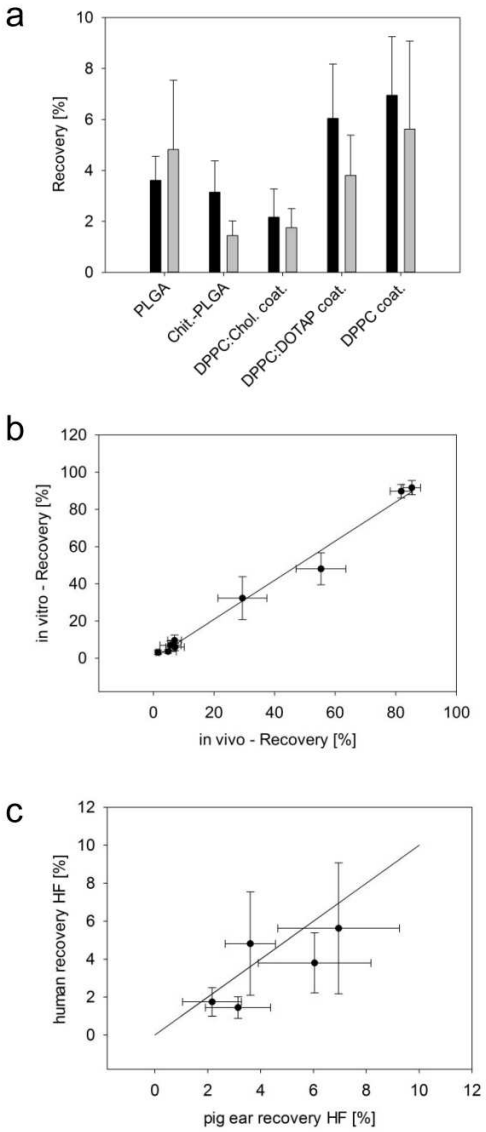

Fig. 5: a: Recovery from the hair follicle of topically applied fluorescence labeled PLGA-,Chit.-PLGA-NP, and NP coated with DPPC:Cholesterol (85 : 15), DPPC:DOTAP (92 : 8) and DPPC (100) in vitro on the pig ear (black bars) and in vivo on the human forearm (grey bars); mean ± SD of n = 8/ 17 for PLGA-NPs in vitro/ in vivo and n = 6/5 for Chit.-PLGA-NPs and PL coated Chit.-PLGA-NPs in vitro/ in vivo respectively. b: IVIVC including the amounts recovered from the skin surface, the HF, the application device and total recovery; mean ± SD and line of identity; r^2 = 0.987 c: IVIVC focusing only on the recovery from the HF, mean ± SD and line of identity

In conclusion, although the pig ear in vitro model slightly overestimated the differences between the NP, the trend that was observed in human volunteers was predicted correctly. Although pig skin is generally considered an appropriate model for topical absorption across human skin and especially with regards to the absorption of particle based formulations, this result could not be expected due to the anatomical differences between human and porcine hair follicles. The dorsal site of the porcine ear is commonly used for skin penetration experiments as it represents the highest similarity to human skin regarding the permeability [74]. On pig ear the number of hair follicles averages 20 hairs per cm^2 [74], in human 18 hairs per cm^2 on the forearm [45]. Although hairs of porcine ear are approximately five times thicker than human vellus hair, it is similar to human terminal hair [74]. Thus the porcine ear provides a skin model suitable to mimic the human forearm in size and number of hair follicles. Valid skin models for the in vitro testing of NP for transfollicular delivery are needed to characterize and to optimize NP as potential drug carries for topical application.

A striking result of the present study was the differences in follicular uptake that we recorded for the different NP. Selectivity for a certain size, charge or chemical features are basic features ensuring meaningful interaction of tissues, cells, or receptors with self and foreign entities. For NP no systematic investigation has been undertaken yet to elucidate this issue as introduced above. By using NP which had very similar hydrodynamic sizes we aimed to investigate the influence of particle material. Keep in mind that hydrodynamic size and zeta potential (i.e. NP mobility in an electric field) are parameters which are measured in highly dilute aqueous dispersion of the particles. Their behavior after application onto the skin is currently a black box which is not trivial to elucidate. Phenomena occurring after topical application of these NP formulation likely include drying, possibly particles aggregate or may interact with the skin surface hydrolipid film as well as the sebum from the HF. Focusing for once on the results obtained in human volunteers in vivo as the gold standard, it is remarkable that plain PLGA NP as well as

DPPC coated and DPPC : DOTAP (92 : 8) coated Chit.-PLGA NP penetrated into the HF to a higher extent than Chit.-PLGA NP and DPPC : Chol. (85 : 15) coated Chit.-PLGA NP (Table 3, Figure 5a). Discussing the plain PLGA and Chit.-PLGA NP separately from the PL coated NP, two separate effects appear. First of all plain PLGA NP were the only NP with a nominally negative zeta potential. It has been shown before by Lee and coworkers that negatively charged NP interact more effectively with the skin surface than positively charged NP, which may explain the higher follicular uptake compared to e.g. positively charged Chit.-PLGA NP [75]. Secondly, we hypothesize that lipid coating or in general lipophilic material properties of NP favor their uptake into the lipid rich environment of the sebum filled HF, as we have seen for the DPPC and DPPC : DOTAP coated NP (Table 3, Figure 5a). This leaves to explain the low follicular uptake of the DPPC : Chol. (85 : 15) coated Chit.-PLGA NP. Cholesterol is known to stiffen lipid bilayers which form the walls of liposomes [76]. Therefore during lipid coating of Chit.-PLGA NP the DPPC : Chol liposomes may spread less effectively on the NP surface, so that the coating is less complete than in the other PL coated NP. Hence, DPPC : Chol. (85 : 15) coated Chit.-PLGA NP are more similar to the Chit.-PLGA NP than the other PL coated NP, which is reflected in their similar low uptake into HF. This hypothesis is further supported by the zeta potential data (Table 1). DPPC coated Chit.-PLGA NP had a lower zeta potential than Chit.-PLGA and DPPC : Chol. (85 : 15)-coated Chit.-PLGA NP reflecting a better coating of the Chit.-PLGA NP and therefore a more effective shielding of the surface charge of chitosan. This effect is masked in the DPPC : DOTAP (92 : 8) coated NP because DOTAP is a positively charged phospholipid, which compensates for the shielding of the charge of chitosan.

We studied uptake into hair follicles of different fluorescently labeled NP and meaningful results were obtained which allow concluding on the best suitable NP system for follicular delivery. As fluorescence labeling was used for quantification, the brightness of the NP fluorescence and the background fluorescence of the matrix determine the analytical constraints of the quantification method. For

labeling with fluorescein it was helpful to use a mixture of ACN : NaOH to enhance the fluorescence intensity. The presented method can easily be modified to be applicable to different carrier systems and issues. Different fluorescent labels may require modifications in the solvent composition and measurement settings. A method transfer to other types of nanoparticles and fluorescent labels was successfully performed in our institute.

The method may further be expanded to drug loaded carrier systems. With the implementation of for example HPLC analytics it would be possible to distinguish between the fate of the NP and the penetration and location of the drug load. As in our study large polymeric NP were used tape stripping was only performed to clean the skin surface from remaining NP formulation but not to sample the SC. If drug loaded NP shall be investigated the number of tape strips can be enhanced to perform depth profiling of the penetrated drug into the SC in parallel. In this case the use of a method to determine the amount of SC removed by each tape strip, e.g. infrared densitometry, or protein quantification, is highly recommended in order to accurately determine the position inside the SC.

3.4 CONCLUSION

Differential stripping was a suitable method to quantify the distribution of five different fluorescently labeled pharmaceutically relevant NP with sufficient sensitivity provided that the fluorescence labeling of the particles is bright enough. The most critical sample when using FITC labeled NP is the cyanoacrylate biopsy of the HF as this sample has the highest matrix background (which will of course depend on the particulars of the analytical method such as the extraction solvent and the quantification method).

Follicular uptake of the tested NP was material dependent. Plain PLGA NP with negative zeta potential and DPPC coated and DPPC : DOTAP (92 : 8) coated Chit.-PLGA NP penetrated into the HF to a higher

extent than Chit.-PLGA NP and DPPC : Chol. (85 : 15) coated Chit.-PLGA NP which may indicate that negative surface charge as well as lipophilic surface properties may facilitate follicular uptake.

The pig ear in vitro model is a suitable model for quantifying follicular uptake. It is well suited to optimize NP based drug delivery systems for follicular drug targeting.

4. INFLUENCE OF APPLICATION TECHNIQUE ON THE UPTAKE OF NANOPARTICLES INTO THE HAIR FOLLICLE

The author of the thesis made the following contributions to this chapter:

Planned, performed and interpreted all major experiments.

4.1. INTRODUCTION

It was shown in the previous chapters that only very small amounts of topically applied NP (less than 10% of the applied amount) penetrate into the HF. The major amount of particles remains on the SC surface which acts as a barrier particles and large cargo-molecules (e.g. vaccine antigens) cannot overcome (Ref). Transfollicular vaccination aims at eliciting a protective immune response via the application of nanoparticle encapsulated antigen (with or without adjuvant) via the HF without impairing the SC barrier function. This aim should be achieved by optimizing the targeting of the deep hair follicle where facilitated penetration conditions and a high density of antigen presenting cells are present. To succeed in transfollicular vaccination the penetration efficiency needs to be optimized. Lademann et al. showed in vitro in the pig ear model that massage enhances the depth of penetration of particles into the follicle [19]. They hypothesized that massage mimics the natural movement of hair in the in vitro model and the hairs act like a gear pump which transports the nanoparticles deeper into the hair follicle.

Using the quantification method described in chapter three it was investigated if the described effect of massage enhances not only the penetration depth but also the amount of NPs taken up into the hair follicle. Fluorescently labeled PLGA NP were applied on pig ears i) without massage, ii) with manual massage using the gloved forefinger and iii) with the help of a mechanic massaging device which also vibrates to investigate whether vibration may be of added value and to achieve a more homogeneous distribution of force.

4.2.MATERIAL AND METHODS

4.2.1. PIG EAR SKIN

Pig ears were obtained from a local abattoir. The ears were removed from the carcass before scalding. After washing and blotting dry with tissue the ears are stored up to two days at 2 – 8°C.

4.2.2. NANOPARTICLES

FITC labeled PLGA-NP as described in chapter 3 were used (average hydrodynamic diameter of 162.8 ± 0.06 nm, size distribution PDI 0.06 ± 0.01, negative zeta potential of - 33.6 ± 2.5 mV, see chapter 3.2.3 and 3.3.1).. Briefly, the particles were prepared by a double emulsion method described in [48]. PLGA NP were stored as freeze-dried powder and re-suspended in dd water to obtain the desired concentration prior to use

4.2.3. APPLICATION PROTOCOL AND SAMPLING

The pig ears were blotted dry with tissue and allowed to dry completely. Hairs were shortened with scissors and incubation sites of 1.767 cm2 were marked with water resistant marker. 15µl of PLGA NP suspension were applied on the application site and i) distributed homogeneously over the incubation site, ii) massaged manually with a gloved forefinger for three minutes or iii) massaged with a vibrating massage device (Mini Massage Stick, Royal Wellness) for three minutes. On each ear one area was treated with each different massage techniques with blank formulation (dd water) to determine the analytical background. 17 areas on 7 ears were treated without massage, 17 areas on7 ears were treated with manual massage and 6 areas on 3 ears were treated with vibration. The pig ears were kept in an incubator at 32 °C without coverage for 1 hour. After incubation the NPs were sampled and analyzed as

described in chapter 3. Briefly, (a) 10 Tape strips were taken to collect NP remaining on the skin surface. (b) Two cyanoacrylate biopsies were performed to collect the cast of the HF which contains the NP penetrated into the hair follicles. (c) A punch biopsy of 4.91 cm^2 including the incubation site was taken to sample NP remaining in the skin rest. (d) Also the application devices (pipette tip for application without massage, glove fingers for application with manual massage and vibration).

4.2.4. SAMPLE EXTRACTION AND ANALYSIS

All samples were extracted in ACN : 0.1 N NaOH (70:30) for three hours under light exclusion and then centrifuged (5 min, 20 °C, 24651 g). Fluorescence intensities of all samples were measured (excitation λ_{ex} = 490 nm, emission λ_{em} = 525 nm) in a plate-reader (TECAN infinite M200, Tecan GmbH, Crailsheim, Germany). For calibration, a stock suspension with known NP concentration (wt/V) was prepared in ACN : 0.1N NaOH (70:30), extracted for three hours and diluted with ACN : 0.1N NaOH to obtain standards.

4.2.5. STATISTICS

Statistical testing was performed by one-way ANOVA with Holm-Sidak all pairwise multiple comparison procedure. A p value of ≤ 0.05 was considered significant.

4.3. Results

Fluorescently labeled PLGA nanoparticles were applied on defined incubation sites on pig ear skin without massage, with manual massage and with a vibrating mechanic massaging device. The fraction of the applied nanoparticles that penetrated into the hair follicles was assessed. Full recovery, which is defined according to the guideline of the within the limits of 100 ± 15%, was found in all experiments. Without massage 26.87 ± 22.87 µg of the applied nanoparticles were found inside the hair follicles which is equivalent to 2.85 ± 2.19 % of the totally applied amount of particles. All results are summarized in Tab. 1. Figure 1 A summarizes the recovery from skin surface, hair follicle, skin rest, application device and the total recovery. Figure 1 B shows the influence of the different application techniques to the uptake into the hair follicle. With manual massage the uptake into the hair follicle increased to 27.00 ± 9.50 µg (3.59 ± 1.26 %). Application with the vibrating massaging device lead to an uptake of particles into the hair follicle of 19.62 ± 8.49 µg (2.54 ± 1.10%). The differences between the application techniques were not statistically significant.

Table 1 NPs recovered from skin surface, HF, and application device and skin rest reported as % (wt/wt) of the total applied dose. Mean ± standard deviation (SD) of n = 17 for performance without massage and manual massage and n = 6 for vibration.

Recovery [%]	Without massage	Manual massage	Vibration
Tape strips	90.04 ± 6.89	53.98 ± 10.86	42.36 ± 7.25
Cyanoacrylate Biopsies	2.85 ± 2.19	3.59 ± 1.26	2.54 ± 1.10
Application device	4.63 ± 1.54	31.60 ± 8.44	40.47 ± 10.48
Total recovery	96.56 ± 6.73	89.11 ± 7.92	88.54 ± 8.28

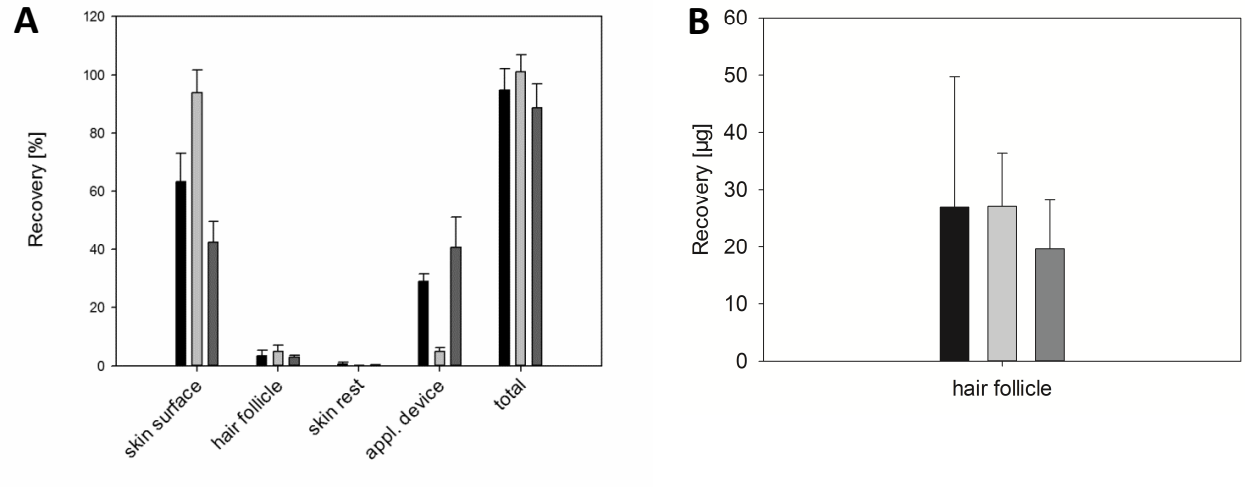

Fig. 1: Recovery of topically applied fluorescently labeled PLGA-NPs from pig ear skin. Particles were applied without massage (black bars), with manual massage (light grey bars) and with vibration (dark grey bars). A: amount of nanoparticles recovered from skin surface, HF, appl. Device and skin rest. B: amount of nanoparticles recovered from the hair follicle. Not statistically relevant difference between the application techniques.

4.4. Discussion

Lademann et. al found that massage enhances the penetration depth of particles inside the HF by analyzing the location of NPs in the HF in histological skin sections without focusing the quantitative aspect[19]. The quantitative impact of the application technique of massage is highly relevant regarding the potential use for tansfollicular application of NPs for medical purposes like vaccination. Massage is described to cause a movement of hairs which makes them act like a gear pump, transporting the NPs deeper into the hair bulb. To differentiate the effect of moving hairs and of vibration both techniques of massage were applied manual massage which only moves the hairs and massage using a vibrating massage device which applies massage additionally to the movement of hairs.

Neither manual nor vibrating massage enhances the uptake into the HF. It can be assumed that the major amount of NP is deposited in the infundibulum of the follicles and only very small amounts penetrate deeper into the follicle [77]. It seems as massage enhances the penetration depth of the fraction of deeply penetrating particles but not its amount. The LLOQ for FITC-labeled PLGA NPs was determined to be 375 µg/ml, which is equivalent to one percent of the applied amount of particles per incubation site. We assume the amount of particles that penetrate deeply into the follicle by the application of massage comes below the limits of the method. As a consequence it can be hypothesized that even if the application of massage has a quantitative effect, it enhances the total uptake into the HF not more than one percent of the applied dose.

4.5. CONCLUSION

To summarize, massage might be an interesting method to support the targeting to deeper regions of the follicle but it is inappropriate to enhance the total amount that can be successfully delivered into the HF. The overall amount of nanoparticles that can be delivered into the hair follicles is thus limited. This limits the application of transfollicular delivery to highly active drugs. It might still be an option for transfollicular vaccine delivery or transfollicular hypodesensitization for curative therapy of allergies

5. NON-INVASIVE DELIVERY OF NANOPARTICLES TO HAIR FOLLICLES – A PERSPECTIVE FOR TRANSCUTANEOUS IMMUNIZATION

Parts of this chapter have been published as:

Ankit Mittal[#], Anne S. Raber[#], Ulrich F. Schaefer, Sebastian Weissmann, Thomas Ebensen, Kai Schulze, Carlos A. Guzmán, Claus-Michael Lehr, Steffi Hansen; Non-invasive delivery of nanoparticles to hair follicles – a perspective for transcutaneous immunization; Vaccine (31) 2013

# the authors contributed equally to this work.

The author of the thesis made the following contributions to the publication:

Planned and designed the manuscript, developed the methodology for all in vitro skin experiments, performed and interpreted all in vitro skin experiments, wrote the manuscript.

5.1. INTRODUCTION

TCI refers to the needle-free application of vaccines across the skin [78]. Major benefits include the possibility of self-administration, improved patient compliance, no requirement of "sharps" waste removal, and reduced storage and transport issues. The skin is a superior organ for eliciting an immune response compared to the muscle due to the abundance of professional APCs such as dendritic cells (DCs) and Langerhans cells (LCs) in different layers of the skin [79, 80]. In addition, TCI can generate both a humoral as well as a cellular response at the site of administration and also at distant mucosal sites [22]. Hence, TCI may allow reducing the antigen dose, as well as eliciting an improved immune response in persons with a disease- or age-compromised immune system [81].

The major challenge for TCI is to enhance the transport of antigens across the stratum SC barrier. To this end often barrier disrupting measures are applied, such as chemical permeation enhancers, abrasion, electroporation, micro-needles, PowderJect, gene gun, etc. [82]. In contrast, transfollicular vaccination aims to deliver antigens to the abundant perifollicular APCs [14, 83]. Any additional barrier disrupting measures should be expendable as the SC only extents into the upper third of the follicle. Solid NPs are the ideal vehicles for transfollicular delivery as they accumulate in HFs and skin folds and penetrate deeper into hair follicles than molecules in solution [56]. Transfollicular delivery has been widely investigated for DNA vaccines, and lately also for non-nucleotide based antigens such as a seasonal flu vaccine as well as NP based formulations

Nonetheless, transfollicular vaccination is usually performed after pretreating the skin area by plucking the hairs, waxing, or cyanoacrylate (superglue) stripping. This pretreatment induces the hair cycle into anagen (proliferation) state and markedly increases the transfection efficiency of follicular keratinocytes [15, 84]. The pretreatment is therefore helpful for DNA vaccines, however, it may be expendable for protein or peptide based antigens. At the same time the SC is (at least partially) removed so that it is not

clear to which extent the antigen penetrates via the hair follicles or across the permeabilized SC. This is especially critical as the reduced barrier increases the risk of pathogen entry which is of particular importance for transfolliclular vaccination in (i) countries with critical hygienic conditions, and (ii) immuno-compromised individuals, such as elderly people with poor wound healing and young children.

This study investigates the potential of transfollicular delivery of OVA using polymeric NPs without compromising the SC barrier by any pretreatment for the purpose of non-invasive TCI. NPs were prepared by a double emulsion method from PLGA or Chit.-PLGA and polyvinyl alcohol (PVA) as stabilizer. These are biocompatible and biodegradable polymers which are widely used for biomedical applications. The NPs were characterized physico-chemically in terms of size, surface charge, OVA encapsulation/loading and morphology. The integrity and biological activity of the encapsulated OVA was monitored by SDS page, *in vitro* proliferation of OVA-specific lymphocytes, and ELISA. The follicular delivery efficiency was measured in intact pig skin based on the differential stripping technique and compared to OVA solution [56, 85]. An adoptive transfer experiment was performed to verify the usefulness of the non-invasive transfollicular immunization route in vivo.

To our knowledge this is the first study to evaluate the potential of transfollicular vaccination using NPs without applying SC barrier reducing measures.

5.2. MATERIALS AND METHODS

5.2.1. MATERIAL

EndoGrade® Ovalbumin (OVA) was obtained from Hyglos GmbH (Bernried, Germany); poly(d,l-lactide-co-glycolide) (PLGA) (Resomer RG 50:50 H; inherent viscosity 0.31 dL/g) was kindly provided by Boehringer Ingelheim (Boehringer Ingelheim GmbH & Co. KG, Ingelheim, Germany); polyvinyl alcohol (PVA) Mowiol® 4-88 was obtained from Kuraray Specialties Europe GmbH (Frankfurt, Germany); ultrapure chitosan chloride salt (Protasan® UP CL113) was purchased from FMC BioPolymer AS (Oslo, Norway); trehalose was obtained from Sigma-Aldrich (St. Louis, MO, USA); fluorescein isothiocyanate conjugated ovalbumin (FITC-OVA) was obtained from Invitrogen (Molecular Probes Inc., Germany). Superglue was kindly provided by Uhu GmbH & Co.KG, (Bühl, Germany). Tesa film was obtained from TESA SE, Hamburg, Germany. The OVA specific ELISA kit was purchased from USCN life science Inc. (Hölzel Diganostik, Germany). All other solvents and chemicals used were of the highest grade commercially available. Deionized water (Milli Q Plus system, Millipore, Bedford, MA, USA) was used throughout the investigation.

5.2.2. PIG EAR SKIN

Ears from freshly slaughtered pigs were removed before scalding. The ears were washed with water, blotted dry and the hairs were shortened with scissors. The ears were stored at 4-8 °C for a maximum period of 3 days.

5.2.3. MICE

Female BALB/c (H-2d) or C57BL/6 (H-2b) mice at the age 6-8 weeks were purchased from Harlan (Germany). OVA-TCR transgenic mice OT-I (C57BL/6-Tg(TcraTcrb)1100Mjb/J), OT-II (C57BL/6-Tg(TcraTcrb)425Cbn), and OT-IIxThy1.1 (C57BL/6-Tg(TcraTcrb)425Cbn Thy1^{a}) were bred at the animal facilities of Helmholtz Centre for Infection Research under specific pathogen-free conditions. The animal experiment permission was given by the local government of Lower Saxony (Germany) with the No. 33.11.42502-04-017/08.

5.2.4. NANOPARTICLES PREPARATION AND CHARACTERIZATION

5.2.4.1. Nanoparticle preparation

PLGA NPs were prepared by a modified double emulsion method [86]. Briefly, 50 mg of PLGA were dissolved in 2 ml of ethyl acetate at room temperature. Then 400 µl of (1.875% wt/V) OVA solution in water was added to form a primary water-in-oil (w/o) emulsion. After sonicating at 6 W for 15 s, 4 ml of 2% (wt/V) PVA solution was added to the primary emulsion and again sonicated at 12 W for 15 s. Water was added drop-wise to the resulting w/o/w emulsion under constant stirring to allow diffusion and evaporation of the organic solvent. The particles were collected by centrifugation at 15,000 g for 10 min, washed once with distilled water to remove excess surfactant and free drug and freeze dried using trehalose (0.2% wt/V) as cryoprotectant.

Chit.-PLGA NPs were prepared in a similar manner as described above with the difference that Protasan® UP CL113 (0.2% wt/V) was added to the PVA solution.

FITC labeled OVA loaded NPs and FITC labeled blank NPs were prepared by replacing OVA or the PLGA polymer with their fluorescent counterparts, respectively.

5.2.4.2. Nanoparticle characterization

Size and ζ-potential of the NPs were analyzed by photon correlation spectroscopy (PCS) using a Nano-ZS (Malvern Instruments, Malvern, UK). The morphology of the NPs was characterized using scanning electron microscopy (SEM) (JSM 7001F Field Emission SEM (Jeol, Japan)) and atomic force microscopy (AFM) (Multimode V (Veeco, USA)). For SEM, prior to scanning, NPs were sputtered with gold (layer thickness approximately 10 nm). The accelerating voltage was 10 kV with a focal distance of 10 mm. For AFM imaging, NPs were scanned using tapping mode and scan rates of 0.6 Hz. A standard non-contact mode cantilever was used for imaging (OMCL-AC160TS, Olympus, Essex, Great Britain).

The entrapment efficiency (% EE = wt OVA encapsulated/wt OVA added initially) and loading efficiency (% L = wt OVA encapsulated/wt polymer) of OVA in PLGA and Chit-PLGA NPs were determined using a QuantiPro bicinchoninic acid (BCA) assay (Pierce, Rockford, IL, USA) according to the manufacturer's instructions for 96 micro-well plates. Briefly, 5 mg of the lyophilized particles were hydrolyzed in 0.1 N NaOH for 6 h and then neutralized with 0.1 N HCl [86]. Blank NPs were used as a control.

5.2.4.3. Integrity and Activity of OVA

The integrity of OVA was determined by SDS PAGE analysis. Briefly, OVA was extracted from freeze-fried NPs under alkaline conditions (0.1 N NaOH). The total amount of protein was quantified using a QuantiPro BCA assay. A dose of 1 µg of OVA was loaded onto a 12% (wt/V) polyacrylamide gel under reducing conditions [87]. Detection of protein was performed by staining with colloidal Coomassie blue (Fermentas, St. Leonrot, Germany).

To determine the activity of OVA encapsulated in NPs 1 ml of each NP dispersion (1 mg/ml) was incubated for 24 h in phosphate buffer (pH 5.5) at 32 °C under continuous stirring at 100 rpm. The dispersion was centrifuged for 20 min at 24,000 g and the total amount of protein in the supernatant was quantified using a QuantiPro BCA assay. Subsequently, the active OVA fraction was quantified using

an ELISA assay which was performed according to the instructions provided by the manufacturer. The ELISA was calibrated using standards provided by the manufacturer in the range of 0.156 – 10 ng/ml (LLOD = 0.053 ng/ml). Supernatant obtained from blank NPs were used as negative control.

5.2.4.4. DC activation and stimulation: Preparation and flow cytometric analysis of murine dendritic cells

Bone marrow-derived primary dendritic cells (conventional DCs) from C57BL/6 mice were generated by flushing femur and tibia of mice with media. Erythrocytes were lysed by adding ACK buffer (0.15 M NH_4Cl, 1.0 M $KHCO_3$, 0.1 mM EDTA, pH 7.2). Cells were washed and incubated on cell culture dishes for up to 2 h. Then non-adherent DC precursors in the supernatant were transferred to 12-well plates (2 x 10^6/well) and differentiated for 5 days in media supplemented with 50 ng/ml GM-CSF. On day 5, DCs were co-incubated with PLGA OVA [10 µg/ml], Chit.-PLGA OVA and different controls, such as PLGA alone for 24 h at 37°C. Control cells were treated with OVA LPS free [10 µg/ml] and OVA co-administered with LPS derived from *Salmonella enterica* Serovar Typhimurium (Invivogene) at a final concentration of 1 µg/ml. For flow cytometry, cells were pre-blocked using anti-mouse CD16/32 antibody for 15 min. Then, DCs were stained with several differentiation and maturation markers conjugated with different fluorochromes, such as CD40 (HM40-3), CD54 (YN1/1.7.4), CD80 (16-10A1), CD86 (GL1), MHC-II M5/114.15.2), and MHC-I (34-1-2S) antibodies (http://www.ebioscience.com/ebioscience/specs/antibody_17/17-5321.html, eBioscience, USA). The FACS analysis of 20,000 events was performed using a LSR-II and the FACSDiva software (BD Bioscience, USA), gating on CD11c positive cells. Results are expressed as mean of three independent experiments, standard error of the mean (SEM) is indicated by vertical lines.

5.2.4.5. Measurement of cellular proliferation of antigen specific murine CD4+ and CD8+ T cells

Differentiated murine DCs were incubated with 10 µg/ml of LPS-free OVA (EndoGrade® OVAlbumin, #321001, Hyglos, Germany), PLGA or PLGA-OVA and Chit.-PLGA or Chit.-PLGA-OVA. After 24h $CD8^+$ T cells derived from spleens of OT-I mice, which have a transgenic T cell receptor specific for the OVA immune-dominant peptide (aa 257-264, SIINFEKL) presented in the context of the MHC class I H-$2K^b$, or $CD4^+$ T cells derived from spleen of OT-II mice expressing the TCR specific for OVA (aa 323–339, ISQAVHAAHAEINEAGR) presented in the MHC class II molecule I-A^b were isolated. Afterwards, the spleen cells were stained with 10 µM carboxy fluorescein succinimidyl ester (CFSE; Molecular Probes, USA) in PBS for 5 min and co-cultured with antigen stimulated murine DCs for 4 days. The loss of CFSE+ labelling of CD8+ and CD4+ T cells in response to stimulation with PLGA-OVA or Chit.-PLGA-OVA were determined by flow cytometry on a BD LSR-II and analysed using the FACSDiva software. Results are expressed as histograms and correspond to one representative experiment out of two independent tests.

5.2.5. Adoptive transfer model of TCR transgenic CD4+ T cells to characterize OVA specific proliferation

Immunization was carried on the flank part of the mice. In brief, 2 d before immunization mice were anesthetized and flanks were shaved using a razor. Shaved areas were carefully inspected for cuts or skin irritation in which case these mice were excluded from the experiment. One day prior to immunization OT-II x Thy1.1 mice derived naïve non-activated OVA-specific CD4+ T-cells (CD4+ CD62Lhi CD44lo CD25-) were isolated and subsequently sorted (purity ≥98%) using an ARIA II sorter (BD Biosciences, San Jose, USA). Then, CD4+ T-cells were labeled with CFSE (10 nM) and transferred to the shaved OVA naïve C57BL/6 mice by tail vein injection (1.5 x 10^6 per mouse). On the day of immunization, mice (n = 4) were immunized: (1) negative control, received Chit-PLGA + 2 µg c-di-AMP as adjuvant dispersed in

physiological buffer via i.m. injection; (2) positive control, received 200 µg / 50 µl LPS-free OVA dissolved in physiological buffer via i.m. injection; (3) received 200 µg / 60 µl LPS-free OVA in Chit-PLGA NPs + 2 µg c-di-AMP as adjuvant via transfollicular application.

Four days post immunization the animals were sacrificed, immune cells were isolated from both spleens and draining lymph nodes (illiac and axillary LNs pooled) and stained (live/dead, CD3+, CD4+ and Thy1.1) separately for each animal. OVA specific proliferation (CFSE dilution) of viable CD3+, CD4+, Thy1.1 cells was analyzed using a LSRII flow.

5.2.6. EVALUATION OF FOLLICULAR UPTAKE ON EXCISED PIG EARS

Incubation sites of 1.767 cm² were marked on the outer auricle of the pig ears with a permanent marker. A dose of 15 µl of either an aqueous solution of FITC-OVA, an aqueous dispersion of FITC-OVA in PLGA NPs, or FITC-OVA in Chit.-PLGA NPs (8.5 µg OVA/cm², 0.16 and 0.13 mg NPs/cm² for PLGA NPs and Chit.-PLGA NPs, respectively) were applied and massaged manually with a gloved forefinger for 3 min. The ears were incubated for 1 h at 32°C under non-occlusive conditions.

5.2.6.1. Microscopical evaluation

Cross-sections of 12 µm thickness were performed on a cryomicrotome (Cryostat Type MEV, Slee, Mainz, Germany). The biopsy was placed in a vertical direction relative to the blade to prevent the spreading of NPs from the skin surface to deeper skin layers. The sections were collected on objective slides, embedded in FluorSave™ embedding medium (Calbiochem®, USA) and sealed with a cover slip.

For the top view image, a skin biopsy was mounted on an objective slide with distance holders and sealed with a cover slip, which immediately touched the skin as well as the distance holders to prevent any skin movement during the imaging process.

Cyanoacrylate biopsies were obtained as described below and fixed on an objective slide.

All samples were imaged under the confocal microscope (Zeiss LSM 510 META system, Carl Zeiss, Jena, Germany). An Argon laser at 458 nm was used to excite the fluorescence signal. As objective a water immersion lens 25X was used. The high auto fluorescence of the skin was excluded by choosing appropriate filters and gain settings. In addition, for the cross-sections and cyanoacrylate biopsies transmission light images were superimposed with the fluorescence images. For top-view and cyanoacrylate biopsy images optical stacks (z-stacks) were performed. Image processing was performed using Volocity® 3D Imaging Analysis Software (Perkin Elmer Inc USA).

5.2.6.2. Quantification of follicular uptake: Influence of encapsulating OVA into particles

After the incubation the skin surface was cleaned from remaining formulation by removing 10 tape strips (Tesa kristallklar, Tesa SE, Germany). A roller was used to enhance the contact between tape strip and skin surface [66]. Subsequently, 2 cyanoacrylate biopsies were performed to collect the amount of OVA penetrated into the hair follicles. The cyanoacrylate biopsies were extracted in ACN : 0.1 N NaOH (70:30) for 3 h on a horizontal shaker and the fluorescence intensity of all samples was measured using a Tecan platereader (Excitation 490 nm, Emission 525 nm). The amount of FITC-OVA extracted from the cyanoacrylate biopsies was calculated with the help of standards prepared from FITC-OVA / FITC-OVA in PLGA NPs / FITC-OVA in Chit-PLGA NPs dissolved in ACN : 0.1 N NaOH (70:30) in the range of 0.1-10 µg/ml. The results for the NPs were expressed relatively to FITC-OVA solution.

Blank samples were taken from an incubation site of the same pig ear; double distilled water was applied instead of NPs. The blank values were subtracted from the fluorescence intensity of the samples.

5.2.6.3. Quantification of follicular uptake: Influence of particle concentration

Follicular uptake was quantified using particle concentrations of 0.22/0.42/0.85 mg NPs/cm². Briefly, 15 µl of each NP dispersion at a concentration of 25/50/100 mg NPs/ml were applied to an area of 1.767 cm² and processed exactly as described above. The NPs used in these experiments were prepared using FITC-PLGA to enable detection and did not contain any OVA. FITC-labeling of PLGA was performed as described in [64]. Standards were prepared from blank FITC-PLGA or Chit.-FITC-PLGA NPS in the range of 5-380 µg/ml dispersed in ACN : 0.1 N NaOH (70:30). Blank samples were taken from an incubation site of the same pig ear; double distilled water was applied instead of NPs. The blank values were subtracted from the fluorescence intensity of the samples.

5.2.7. STATISTICAL ANALYSIS

Statistical analysis was performed by a one-way ANOVA. A p value of ≤ 0.05 was considered significant.

5.3. RESULTS

5.3.1. CHARACTERIZATION OF NANOPARTICLES

The SEM and AFM images in Fig.1 show smooth, spherical particles. The characteristics of the NPs are summarized in Table 1. The mean size of OVA loaded PLGA and Chit.-PLGA NPs was ca. 170 nm and 180 nm, respectively, with a monodisperse size distribution (PDI < 0.2). PLGA NPs have a negative surface charge whereas Chit.-PLGA NPs have a positive surface charge. Antigen incorporation into PLGA and Chit.-PLGA NPs slightly increased the particle size and reduced the overall surface charge compared to blank NPs. For both particle types similar %EE of 27.61 ± 2.52% and 36.54 ± 2.44% and %L of 5.43 ± 0.47% and 6.65 ± 0.44% were obtained (for PLGA and Chit.-PLGA NPs respectively).

Table 1 Physico-chemical characterization of the optimized PLGA and Chit.-PLGA NPs Values represent mean ± standard error of the mean (SEM) of n = 6 independently prepared batches, except for %A where n = 3. Z.P. zeta potential, %EE encapsulation efficiency (wt OVA encapsulated/wt OVA added initially), %L loading (wt OVA encapsulated/wt polymer), %A activity (wt OVA active/OVA encapsulated)

Nanoparticle	**Size (nm)**	**PDI**	**Z.P. (mV)**	**% EE**	**% L**	**%A**
Blank PLGA	162.8 ± 1.66	0.056 ± 0.005	-31.5 ± 1.03	-	-	
OVA loaded PLGA	168.5 ± 1.45	0.063 ± 0.008	-24.8 ± 0.89	27.61 ± 1.03	5.43 ± 0.19	73.59 ± 2.91
Blank Chit-PLGA	171.5 ± 1.36	0.123 ± 0.012	24.1 ± 0.78	-	-	
OVA loaded Chit-PLGA	183.6 ± 2.71	0.171 ± 0.012	20.2 ± 1.05	36.54 ± 1.08	6.65 ± 0.18	63.57 ± 2.68

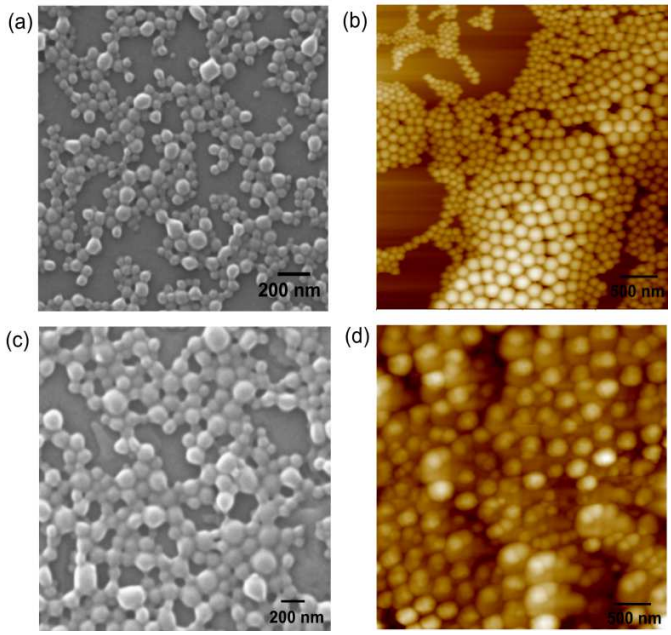

Fig. 1: Top: (a) & (b) SEM and AFM images of OVA loaded PLGA NPs; bottom: (c) & (d) SEM and AFM images of OVA loaded Chit.-PLGA NPs

5.3.2. INTEGRITY AND ACTIVITY OF OVA

To investigate the formation of fragments or aggregates of OVA during NP preparation, an SDS PAGE was performed. Weak differences in the migration pattern of OVA extracted from NPs compared to control (OVA in aqueous solution) were observed as shown in Fig. 2(a). While no fragments were obtained, low amounts of higher molecular weight adducts, probably dimers and trimers (ca. 95 and 135 kDa), were observed in the case of OVA extracted from NPs. Lanes 3 and 5 (blank NPs) show that no interference from the NP formulations is to be expected.

In addition, ELISA was performed using the OVA which had been extracted from the NPs. By relating the result to the total amount of protein in the sample the activity of the encapsulated OVA was determined as 74% and 64% in PLGA and Chit.-PLGA NPs, respectively (results not shown).

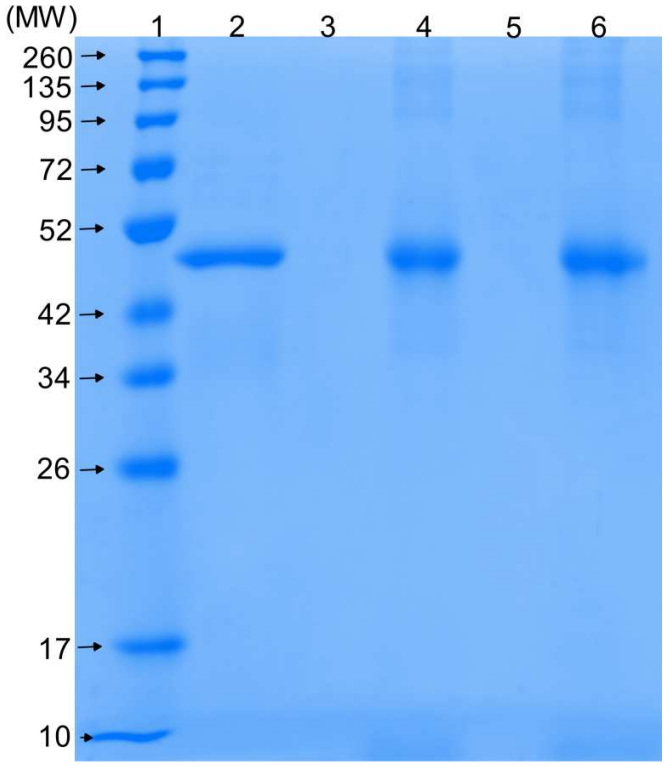

Fig. 2: Integrity of OVA extracted from NPs by 0.1 N NaOH and analyzed by SDS PAGE, Lane 1: MW standards, Lane 2: OVA control, Lane 3: Blank PLGA, Lane 4: OVA extracted from PLGA NPs, Lane 5: Blank Chit-PLGA, Lane 6: OVA extracted from Chit-PLGA NPs

5.3.3. ACTIVATION OF DENDRITIC CELLS

We analyzed the effect of PLGA-OVA and Chit.-PLGA-OVA on the activation and maturation of bone marrow-derived murine DCs. Both, PLGA-OVA and Chit.-PLGA-OVA were able to promote an efficient activation and maturation of DCs in vitro when used at a final OVA concentration of 10 µg/ml (Fig. 3). Changes in the activation markers (% of CD11c+ DCs indicates the number of activated DCs; mean fluorescence intensity (MFI) indicates the expression level of a certain marker per cell) were modest but except for CD54 an increase compared to negative control was detected for all NP groups as well as for OVA alone (Fig. 4). Interestingly, no significant differences in the expression levels of activation markers

have been observed comparing values of DCs stimulated with OVA alone with those of DCs incubated in the presence of any NP formulation (Fig. 4). In general incubation of DCs in the presence of OVA alone and in combination with LPS stimulated similar changes in activation markers except for CD40 and CD80 where the addition of LPS increased the marker expression per cell (Fig. 4).

However, we next evaluated the capacity of APCs loaded with antigen in presence of PLGA-OVA and Chit-PLGA-OVA to stimulate the proliferation of antigen-specific CD8+ and CD4+ T cells. DCs stimulated with OVA loaded Chit.-PLGA NPs were able to induce a strong antigen-specific proliferation of CD8+ T cells (67.5%) from OT-I mice, as shown by the loss of CFSE+ stained cells (Fig. 3, left column). Furthermore, theses DCs were also able to stimulate the proliferation of CD4+ T cells (95.6%) derived from OT-II mice (Fig. 3, right column). Nevertheless, weaker T cell proliferation was also observed when DCs were stimulated with OVA LPS-free alone (21 and 68%, for OT.I and OT-II respectively) (Fi.g 3). DCs stimulated with OVA loaded PLGA NPs were also able to stimulate the proliferation of OT-I and OT-II cells although to a lesser extend compared with OVA alone and the OVA loaded Chit.-PLGA NPs (10 and 95%, respectively) (Fig. 3). OVA free NPs promote only very marginal DC activation/ T-cell proliferation if any at all (Fig. 3). Interestingly, LPS induced only week CD4+ T cell proliferation compared to OVA and PLGA-OVA and Chit.-PLGA-OVA (Fig. 3)

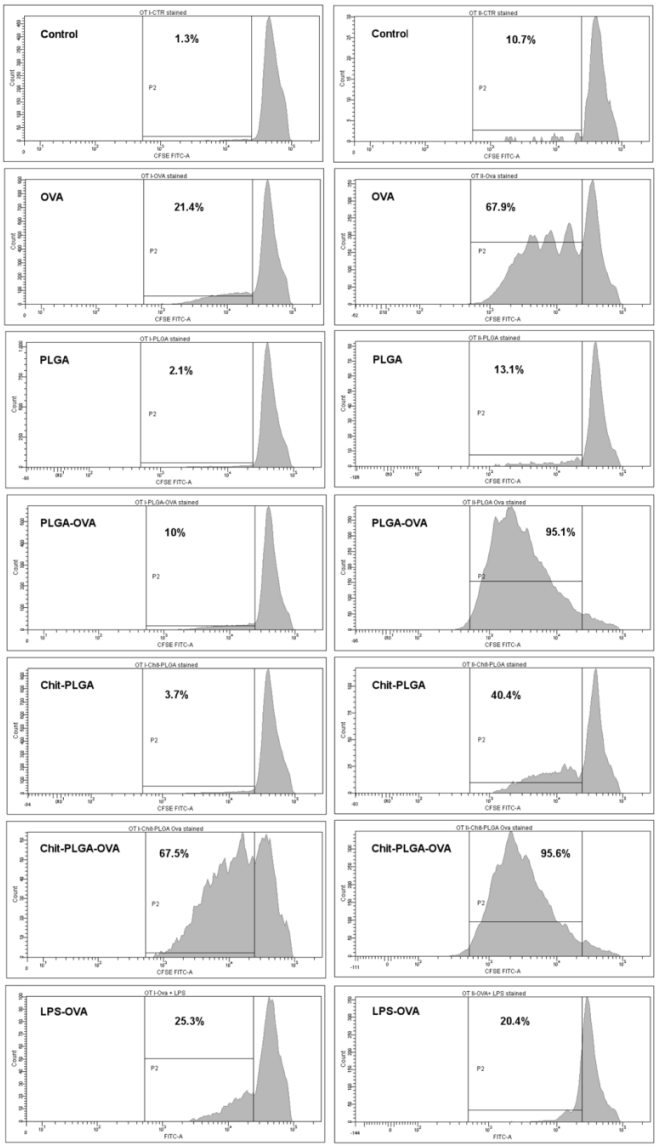

Fig. 3: Ova-specific proliferation of OT-I (left panel) and OT-II lymphocytes (right panel) stimulated by NP-OVA pulsed DCs. Bone marrow-derived DCs were incubated for 24 h in the presence of OVA LPS free [10 µg/ml], PLGA, PLGA-OVA [10 µg/ml], Chit.-PLGA and Chit.-PLGA-OVA [10 µg/ml], respectively. Non-stimulated pulsed DCs were used as negative control. Then, the loaded DCs were co-cultured with either CFSE labeled naïve CD8+ or CD4+ T cells derived from OT-I and OT-II mice, respectively, for 4 days and further analyzed by flow cytometry. The results are representative out of two experiments and are expressed as histograms showing the percentage of proliferating OVA-specific T cells of all CD8+ (OT-I) and CD4+ (OT-II) T cells, respectively.

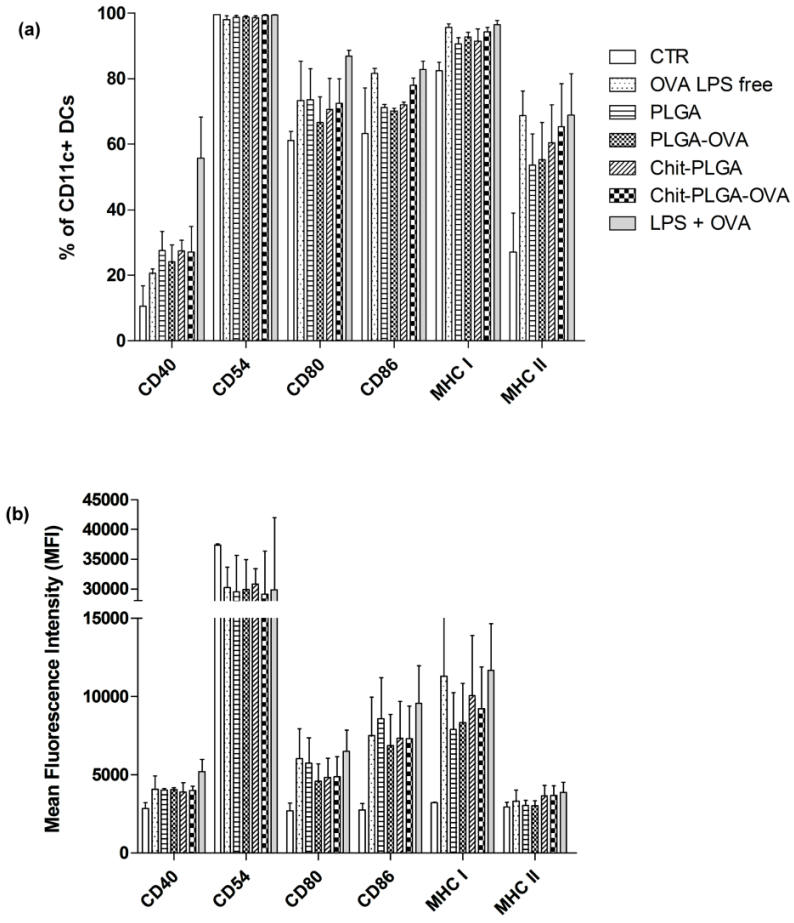

Fig. 4: Expression of activation marker by murine DCs after stimulation with PLGA-OVA and Chit.-PLGA-OVA. The expression of surface markers on $CD11c^{+}$-gated bone marrow-derived murine DCs following stimulation with OVA LPS free [10 µg/ml], PLGA, PLGA-OVA [10 µg/ml], Chit.-PLGA and Chit.-PLGA-OVA [10 µg/ml], respectively, was investigated by flow cytometry. After 24 h of incubation DCs were stained with Abs specific for CD40, CD54, CD80, CD86, MHC-I and MHC-II molecules and analyzed by flow cytometry (BD LSR-II). Results are mean ± SEM of three independent experiments and expressed as percentage (a) and mean fluorescence intensity (MFI) (b), respectively, of CD11c+ cells.

5.3.4. *Adoptive transfer model of TCR transgenic CD4+ T cells to characterize OVA specific proliferation*

In order to verify the feasibility of transfollicular immunization as alternative vaccination strategy, an adoptive transfer model was established. Proliferation of adoptively transferred OVA specific CD4+ T cells was measured by CFSE dilution in the draining lymph nodes and secondary lymphatic organ.

The number of divided OVA specific CD4+ T cells is shown in Fig. 5 (one representative animal of 4 animals per group). As expected no proliferation of transferred cells isolated from draining lymph nodes have been observed in the negative control (Fig. 5a), whereas animals of group 2 (immunized i.m. with OVA protein as positive control) showed a strong proliferation (95.9% of the transferred cells proliferated for up to seven divisions, Fig. 5b). Mice immunized by transfollicular application of Chit.-PLGA-OVA co-administered with c-di-AMP as adjuvant showed a comparable proliferation potential (96.2%) and divided up to nine times (Fig. 5c).

Fig. 6 shows the percentage of divided transferred cells for each experimental group. The four animals of each group were analyzed separately. While no proliferation was observed in the negative control (group 1), full proliferation of the transferred cells was observed in animals of the positive control group (group 2) and in animals immunized transfollicularly with Chit.-PLGA-OVA and c-di-AMP as adjuvant (group 3). An adoptive transfer experiment demonstrated that the model antigen OVA can be delivered via the transfollicular route. This preliminary experiment is a proof of concept that by this transfollicular immunization approach it is possible to deliver antigens, thereby stimulating antigen-specific T cells.

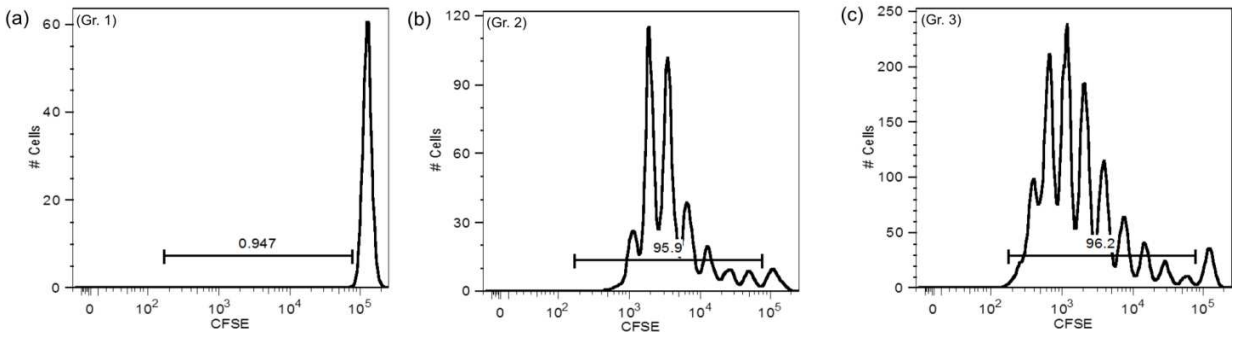

Fig. 5: Animals of group 1 were immunized with empty Chit-PLGA NPs and the adjuvant c-di-AMP i.m. As expected no proliferation of transferred cells was observed in this negative control (A). Animals of group 2 were immunized i.m. with OVA protein as positive control. More than 95% of the transferred cells proliferated after this stimulation (B). The mice of group 3 were immunized by transfollicular application of OVA loaded Chit.-PLGA NPs and c-di-AMP as adjuvant which led to proliferation comparable to the positive control (C). Shown is the proliferation of cells isolated from draining lymph nodes of one representative animal per group.

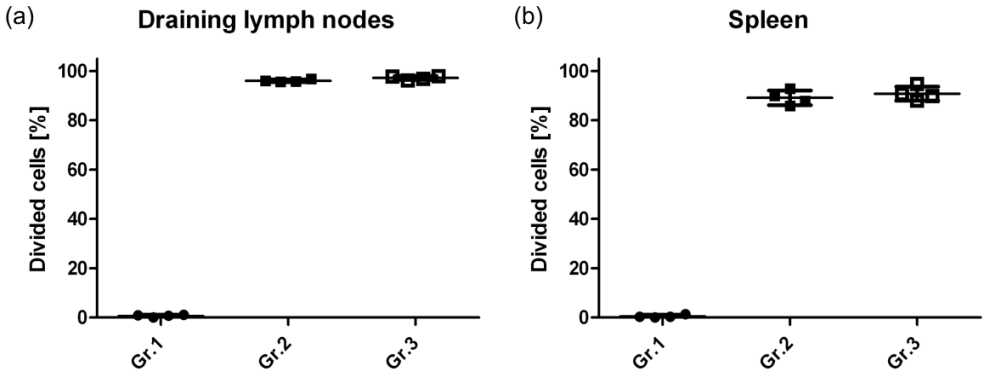

Fig. 6: The percentage of divided transferred cells in the draining lymph nodes (a) and the spleen (b) for each experimental group is shown. The four animals of each group were analyzed separately. While no proliferation was observed in the negative control (Gr. 1), full proliferation of the transferred cells was observed in animals of the positive control group (Gr. 2), and in animals immunized transfollicularly with Chit.-PLGA-OVA and c-di-AMP as adjuvant (Gr. 3). This experiment demonstrates that the model antigen OVA can be delivered via the transfollicular route and that the immunization by this route is able to elicit the same proliferation of OVA specific CD4+ T cells as the i.m. injection of OVA.

5.3.5. FOLLICULAR UPTAKE OF NANOPARTICLES

Fig. 7 shows representative images illustrating the distribution of fluorescently labeled NPs on the skin surface and in the hair follicle after application to excised pig ears. From both the cross-section as well as the top-view it is apparent that the NPs accumulated in the follicle openings, cover the hair and invade into the follicular duct (Fig. 7 (a,b)). Fig. 7c shows a cyanoacrylate biopsy of the follicular content, which further confirms the presence of NPs inside the hair follicles.

By extracting cyanoacrylate biopsies with organic solvents and quantifying the fluorescence in the extract the uptake into the follicles was quantified (Fig. 8). Encapsulation of OVA into NPs significantly enhanced follicular uptake of OVA by a factor of 2.85 ± 0.6 (FITC-OVA in PLGA NPs) and 2.33 ± 0.52 (FITC-

OVA in Chit.-PLGA NPs) compared to OVA solution (Fig. 7a). Follicular uptake of OVA was slightly lower for Chit.-PLGA compared to PLGA NPs, however, this difference was not significant (Fig. 8a).

Furthermore, using FITC-labeled PLGA it turned out that follicular uptake of particles is a function of the NP dose/area relation. Thus the uptake can further be enhanced by increasing the NP concentration in the formulation (Fig. 8b).

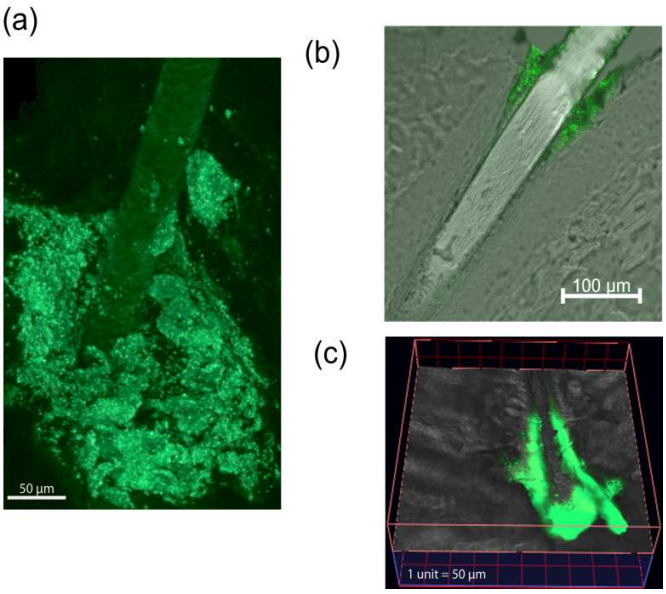

Fig. 7: Distribution of fluorescently labeled NPs in hair follicles after application to excised pig ears. (LSM 510 Meta, Carl Zeiss GmbH, Jena Germany; excitation wavelength 458 nm)

(a) Top view onto the skin surface – image reconstituted after optical sectioning (41 individual frames of 3 µm thickness): NPs accumulate in the follicle opening. The hair is visible as a negative image due to NPs on the hair surface.

(b) Transversal cryo section (thickness 12 µm); overlay of fluorescence and transmission light images: NPs are visible on the skin surface and inside the follicle.

(c) Cyanoacrylate biopsy – one plane selected from optical sectioning (section thickness 0.5 µm); the position of the plane relative to the entire optical stack can be estimated from the height of the box; overlay of fluorescence and transmission light images; the skin surface is oriented towards the bottom of the image: NPs are visible deep inside the cyanoacrylate biopsy which was performed to extract the follicular content.

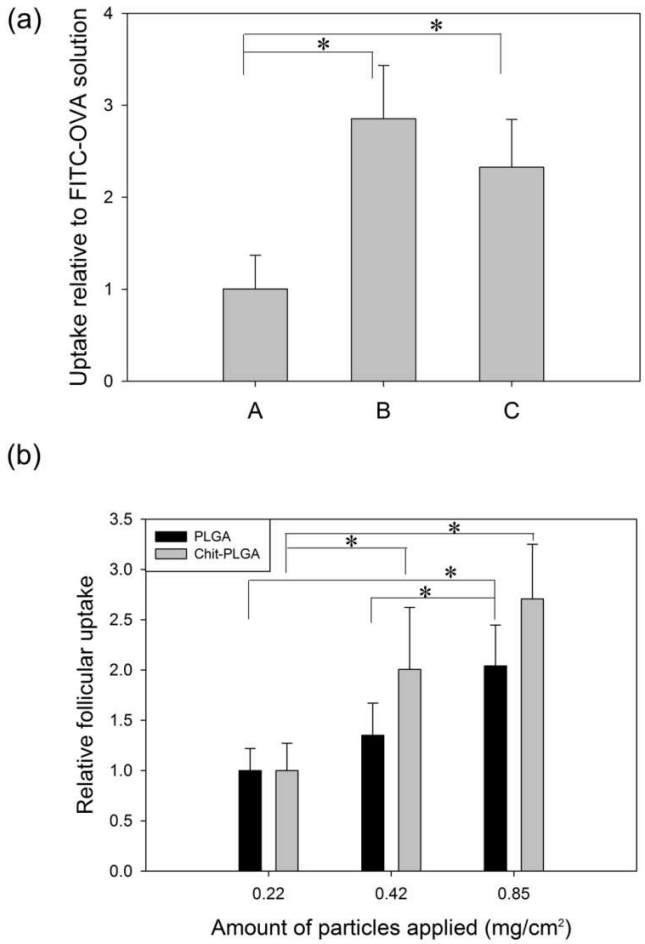

Fig. 8: (a) Uptake of FITC-labeled OVA encapsulated in NPs relative to FITC-OVA solution A: FITC-Ova solution, B: FITC-OVA in PLGA NPs, C: FITC-OVA in Chit.-PLGA NP. (applied dose: 8.5 µg OVA/cm², 0.42 mg NPs/cm²; n = 6, mean ± SEM; * indicates significant differences compared to A with $p < 0.05$)

(b) Effect of NP concentration on follicular uptake. The results are expressed relatively to the lowest NP concentration. (n = 3 except for the highest conc. measured with Chit.-PLGA NPs where n = 2, mean ± SEM; * indicates significant differences compared to the lowest NP concentration with $p < 0.05$)

5.4. DISCUSSION

Transfollicular delivery of antigen by using NPs holds the potential for TCI without the need to weaken the protective SC barrier. So far, studies demonstrating transfollicular antigen delivery used additional barrier disrupting methods such as tape stripping, plucking or intense skin hydration [15, 88, 89]. We hypothesize that by encapsulating the antigen into NPs transfollicular vaccination can be optimized, benefiting from the unique properties of such nano-formulations which should finally allow the application without any barrier disrupting measures. Most NPs cannot overcome the intact SC except for ultrafine particles (< 10 nm, consequently suffering from an extremely low loading capacity) and ultra-flexible liposomes [79]. However, once the particles are located deep inside the hair follicles the SC is no longer an obstacle towards penetration. It has already been demonstrated (although only in mice) that 200 nm particles can be taken up by perifollicular APCs [88, 89]. In fact, transfollicular vaccination by using NPs to encapsulate the vaccine antigen imitates the natural route of delivery observed for pollen allergens in patients suffering from atopic dermatitis. Pollen grains are micron-sized particles which accumulate in the follicle openings and release the allergen after getting into contact with sweat [13, 90]. Also, upon depletion LCs quickly re-populate the epidermis within a period of 24 h, the primary source for LCs being the hair follicles [91, 92].

In this study we prepared polymeric NPs from PLGA and/or chitosan. Both polymers are widely used for drug delivery purposes, especially for preparing depot formulations with a sustained bioavailability of protein and peptide drugs [93-95]. Chitosan and its derivatives are widely used as non-viral vectors for nucleotide based drugs as these are easily complexed by the positively charged polymer [96, 97]. Both polymers are “generally regarded as safe” (GRAS), biocompatible and biodegradable. Chitosan furthermore has mucoadhesive properties, facilitates permeation, and has intrinsic adjuvant properties [98, 99].

Encapsulation into NPs can help to stabilize protein based antigen, modify the release, and improve uptake by APCs [100-102]. At the same time the NP preparation process itself threatens protein integrity and bioactivity due to exposure to organic solvents, interfacial tension, and high shear forces [103]. Liquid/liquid and solid/liquid interfaces occur during all steps of protein encapsulation, protein release and storage and may cause conformational changes and/or aggregation. Apart from losing therapeutic activity aggregates may cause unpredictable side effects and lead to immunogenicity or toxicity [95]. During storage these issues may be minimized by freeze-drying. However, upon reconstituting the lyophilisate and during drug release degradation of PLGA will create an acidic microenvironment which leads to acidic hydrolysis of protein antigens [104, 105]. For comparison, commercially available preparations of BSA usually contain 5-20% of covalent multimeric water soluble aggregates [106]. We could show that 74% and 64% of OVA released from PLGA and Chit-PLGA NPs respectively bind to a monoclonal antibody. This allows a conservative estimate of the activity of the released OVA as at least the epitope recognized by the primary antibody in the ELISA has to be intact. Our results show that despite the formation of aggregates during particle preparation the activity of OVA was largely retained. In other words, by applying a usual dose of 8.5 µl NP suspension per cm² (50 mg NPs/ml, 54.3 ± 0.047 and 66.5 ± 0.044 µg OVA/mg NPs, 74% and 64% activity, for PLGA and Chit.-PLGA NPs respectively) an effective dose of 17 µg/cm² (PLGA) or 18 µg/cm² (Chit.-PLGA) of active OVA is administered considering the measured loading efficiency and activity of the encapsulated OVA.

Using OVA loaded PLGA and Chit.-PLGA NPs for the stimulation of DCs demonstrated that these particles exhibit the capacity to activate murine DCs *in vitro* (Fig. 4). This is a critical step for the development of immune interventions based on NPs, since activation and maturation of DCs is recognized as a key event in the stimulation of adaptive immune responses [107]. Only marginal differences have been observed comparing the expression levels of activation markers by DCs stimulated with OVA alone and OVA loaded NPs (Fig. 4). Only the number of MHC class II molecules seems to be slightly increased on DCs

stimulated with Chit.-PLGA formulations compared to those stimulated with OVA alone. This may be due to the influence of regulatory T cells present in the OT splenocyte preparation which was used to for the co-culture with DCs [108].

Interestingly, following co-incubation of bone marrow derived DCs with OVA and LPS only CD40 expression was increased compared to DCs stimulated with OVA alone, whereas in case of all other investigated markers only marginal differences have been observed (Fig. 4). In addition, also the capacity of LPS stimulated DCs to promote T cell proliferation was marginal (Fig. 3). One possible explanation might be a contamination of the assay with IL-10 which was shown to inhibit the expression of TLR4 by DCs which subsequently prevents their activation by the TLR4 agonist LPS [109]. The source of IL-10 could be bone marrow-derived macrophages which were left in the DC population prepared from murine bone marrow and which were shown to produce IL-10 by stimulation with LPS [110].

Nevertheless, DCs stimulated with OVA loaded NPs were able to stimulate a strongly enhanced clonal expansion of OVA-specific CD4+ OT-II cells compared to those stimulated with OVA protein alone. However, only Chit.-PLGA NPs were able to also promote an enhanced proliferation of OVA-specific CD8+ OT-I cells (Fig. 3). An obvious difference between PLGA and Chit.-PLGA NPs which both have similar size/shape/OVA loading/Ova stability is their opposing surface charge (Table 1). This leads to conclude that the positive particle charge, which generally improves cellular adhesion, internalization, and endosomal escape, may be a reason for the superiority of the Chit.-PLGA NPs to promote CD4+ and CD8+ proliferation [111]. A preferred stimulation of CD8+ T cells may further be expected upon transfollicular application [17, 88]. Antigen uptake by DCs and induction of DC maturation by Chitosan and PLGA NPs has been investigated by other groups as well but shows inconclusive results, unfortunately also concerning the absence [112] or presence of an effect of particle surface charge [113]. This indicates that in addition to the surface charge also the composition of the NPs may play a role [114, 115]. The composition (e.g. degree of substitution, chain length) of the biopolymer chitosan depends on the source

of manufacturer as well as varies from batch to batch which makes it difficult to compare between studies.

The adoptive transfer model is a well-established tool to characterize T cell activation in vivo, since TCR-transgenic mice are tolerogenic to their TCR specific antigen (reviewed in [116]). In the present study adoptive transfer experiments were performed to analyze the transfollicular vaccination route in comparison with the i.m. route in an *in vivo* setting. Transfollicular immunization and subsequent analysis of the triggered immune responses in the draining lymph nodes and secondary lymphatic organ four days after immunization appealed as the most suitable technique to assess proliferation of the transferred cells. Indeed, transfollicular administered OVA in Chit.-PLGA NPs + c-di-AMP as adjuvant elicited strong OT-II cell proliferation. The fact that more cell divisions were observed after transfollicular administration of Chit.-PLGA-OVA NPs compared to those observed following i.m. administration of OVA alone provides evidence that combination of OVA with NPs activated the OVA-specific cells more efficiently which resulted in enhanced proliferation. Future immunization studies with disease relevant antigens need to show whether a potent immune response can be elicited by transfollicular vaccination without the use of barrier disrupting methods. It should be kept in mind that secondary to permeabilizing the skin, tape stripping or other barrier disrupting methods activate the innate immune response and thus work as an unspecific adjuvant. This includes the secretion of the proinflammatory cytokines TNF-α, IL-1α, IL-1β, and GM-CSF by keratinocytes. TNF-α and IL-1β trigger the upregulation of the expression of a6 integrins, intercellular adhesion molecule 1 (ICAM.1), CD86 and MHC class II molecules which then promote the dissociation of LCs from keratinocytes, their subsequent maturation and migration, and improves the antigen-specific immune responses [22, 91, 117]. The use of immune-stimulating molecules or adjuvants in the formulation is an alternative to further optimize the elicited immune responses. This may become important to overcome the tolerogenic potential of the perifollicular LCs and dermal DCs. Mattheolabakis et al. showed that TCI with OVA encapsulated in

poly(lactic acid) NPs was less immunogenic than soluble OVA, however by the addition of the adjuvant cholera toxin boosted the immunogenicity of the NP formulation over that of soluble antigen [118].

While the immunological response towards vaccines is foremost evaluated in different mouse models, rodent skin is not appropriate for testing transdermal delivery and especially transfollicular penetration. Mouse SC has a different corneocyte architecture as well as lipid composition and arrangements, leading mouse skin to be more leaky and therefore an inappropriate surrogate for transdermal delivery in man [119]. With special regards to their hairs, mice have a higher follicular density than man while pig and man resemble each other more closely (mouse: >5000/cm², pig: ca. 22/cm², human ca. 25/cm² on the forearm) [120, 121]. Due to the limitations the mouse model represents, we also investigated the delivery of nano-encapsulated OVA to terminal follicles on the porcine ear. Pig skin is an appropriate substitute for human skin, pig ears are the gold standard model for investigating follicular penetration [82, 122]. The ear cartilage prevents tensile fibers from irreversibly closing the follicle openings which drastically reduces follicular uptake in excised human skin [123].

For transfollicular vaccination it will be essential that the delivery efficiency into the hair follicle is high, i.e. that major parts of the dose are delivered to the peri-follicular APCs. We observed the distribution of the NPs on the skin surface and within the follicular duct (Fig. 5). The real invasion depth into the follicle remains elusive from these images as only the upper part of the follicle is visible in the cross-section. It requires an extensive number of consecutive cuts to obtain reliable measurements due to the angular orientation of the hairs inside the skin [11, 124]. We observed 2-3 times higher drug amounts in the hair follicles if OVA was encapsulated in NPs compared to solution. The follicular uptake efficiency could further be increased by increasing the NP dose/area. No significant differences were observed in the follicular uptake of PLGA and Chit-PLGA NPs (Fig. 7a). Both NPs have a similar size and size distribution but opposite surface charges. These results are in line with the study by Patzelt et al. who suggested that the invasion depth into the follicles depends foremost on NP size and less on particle surface properties

[11]. In general, follicular uptake of microparticles is preferred [125]. For terminal hairs in pigs the optimum particle size for deep penetration was found to be 650 nm [11, 124]. The data presented in this work further underline the great potential of NPs to improve transfollicular vaccination as compared to administering the “naked” antigen across the intact SC.

5.5. CONCLUSION

In conclusion OVA protein could be incorporated with only moderate loss of biological activity into NPs made from PLGA and Chit-PLGA. Encapsulation increases the delivery of OVA to the follicle by a factor of 2 to 3 and can be further increased by increasing the dose of particles applied by area. No pretreatment such as plucking the hairs, waxing or superglue stripping was required to achieve a follicular uptake so that the SC barrier was left intact. Deep penetration into the follicles by the help of NPs delivers the antigen into the vicinity of the perifollicular APCs. OVA loaded PLGA and Chit.-PLGA NPs were able to stimulate efficiently murine DCs and subsequently antigen-specific CD4+ and CD8+ T-cells. An adoptive transfer experiment demonstrated that the model antigen OVA can be delivered via the transfollicular route. This preliminary experiment is a proof of concept that by this transfollicular immunization approach it is possible to deliver antigens, thereby stimulating antigen-specific T cells. Thus, transfollicular delivery seems a promising opportunity vaccination strategy under critical hygienic conditions, for example in individuals with impaired immune system or the elderly.

SUMMARY

In this thesis the uptake of NPs into the HF was investigated with particular regard on quantity, to estimate the potential of NPs as drug carriers for transfollicular drug targeting, especially for transcutaneous vaccination.

Based on the differential stripping technique a method was developed to quantify NP uptake into HF and applied in vitro in a pig ear model and in vivo in human volunteers. An excellent in vitro-in vivo-correlation of $r^2 = 0.987$ between both models was demonstrated, supporting the suitability of the pig ear model as a surrogate for the in vivo situation in humans for quantifying NP uptake into HF.

The influence of NP material on HF uptake was investigated using fluorescence labeled PLGA NP with different surface modifications: i) plain PLGA, ii) chitosan-coated PLGA, and iii) Chit.-PLGA coated with different PL (DPPC (100), DPPC : Chol (85:15), and DPPC : DOTAP (92:8)). The samples were extracted for fluorescence quantification in a mixture of ACN : NaOH. NPs coated with DPPC (100) and DPPC : DOTAP (92:8) penetrated into the HFs to a higher extent than the other tested nanoparticles. The effect was observed both in the pig ear model as well as in human volunteers.

Only a small amount of topically applied NP penetrated into HFs, for transcutaneous vaccination it is essential to achieve the highest possible delivery efficiency. From literature it is known that NPs applied with massage penetrate deeper into the follicle compared to application without massage. Using the new quantification method it was investigated if application techniques like manual massage or vibration can enhance the amount of NPs delivered to the HF. Fluorescently labeled PLGA-NPs were applied on the pig ear model with i) without massage, ii) with manual massage with the gloved forefinger, iii) with a

vibrating massage device. However neither manual massage nor massage with a vibrating massage device were able to enhance the delivery efficacy significantly.

Furthermore it was demonstrated that the usage of NP formulations instead of solutions enhances the deliver efficacy into the hair follicles. In the pig ear model the encapsulation in NP increased the follicular delivery of OVA by a factor of 2 – 3 compared to OVA solution. Increasing amount of NP applied onto skin may additionally increase the delivery efficiency by a factor of ~ 2 – 2.4.

In a proof-of-concept study PLGA and Chit.-PLGA NPs were prepared with OVA as model antigen. OVA was successfully incorporated into the particles with only a moderate loss of biological activity. In a cell culture assay OVA loaded NPs stimulated the proliferation of CD4+ and CD8+ T-cells to a larger extent than OVA in solution. An adoptive transfer experiment in mice demonstrated the successful antigen delivery and immunization via the transfollicular route. With this preliminary experiment it was shown that transfollicular antigen delivery and immunization using nanoparticles as carrier system is possible.

In summary transfollicular vaccination using NPs as vaccine carriers is a promising approach. The main challenge is to deliver a sufficient dose of antigen. Currently the major amount of applied antigen is lost on skin surface without being delivered to the immune system. Though promising results could be achieved the loss of antigen is not in line with dose sparing concepts. Future research should focus on the optimization of the carrier systems to enhance the targeting efficiency.

The results of the proof of concept study in the mouse model were encouraging. Transfollicular vaccination studies in vivo should be expanded from the model antigen OVA in the mouse model to clinically used antigens like influenza vaccines and also be tested in different animal models. Due to the tremendous higher number of HF/cm² compared to human, the mouse model is only of limited

suitability. Encapsulating approved antigens in NPs made of FDA approved biodegradable and biocompatible polymers like PLGA even clinical trials in human could be feasible in the near future.

The quantification method could help to develop carrier systems with enhanced penetration efficiency to the HF. The influence of the PL coatings was a first step to investigate uptake influencing parameters. Quantifying the penetration of NP into the hair follicles can be relevant for dose finding experiments not only for TCI but for follicular targeting in general. Using drug loaded carrier systems, the fate of the nanoparticles and the fate of the drug could be monitored simultaneously. The method can easily be modified with different analyzing methods like HPLC for example. Furthermore a combination with well-established sampling techniques like tape stripping would be useful, especially if the hair follicle is used as target side. Already tape stripping is part of the sampling procedure with intention to clean the skin surface from remaining NP. Increasing the number of tape strips would allow performing a depth profile of the drug penetrated into the SC in parallel. Especially development and bioequivalence testing of therapeutics for hair follicle related disorders like acne or alopecia could benefit of this method.

ZUSAMMENFASSUNG

In dieser Arbeit wurde die Aufnahme von Nanopartikeln in Haarfollikel untersucht, wobei das Hauptaugenmerk auf die Quantität der Aufnahme gelegt wurde. Hierdurch sollte die Eignung von polymerischen Nanopartikeln als Arzneistoffträger für die transfollikuläre Anwendung, besonders die transfollikuläre Vakzinierung ermittelt werden.

Basierend auf der Methode des differenzierten Strippings wurde eine Methode entwickelt um die Aufnahme topisch applizierter Nanopartikel in die Haarfollikel quantitativ zu bestimmen. Diese Methode wurde erfolgreich im Schweineohr-Modell in vitro und am Menschen in vivo angewandt, wobei eine hervorragende in-vitro-in-vivo-Korrelation von $r^2 = 0.987$ zwischen den beiden Modellen ermittelt wurde. Die Eignung des Schweineohr-Modells als Surrogat für die in vivo Situation am Menschen konnte somit auch für quantitative Untersuchungen am Haarfollikel belegt werden.

Der Einfluss des Materials der Nanopartikel auf die Aufnahme in Haarfollikel wurde mit Hilfe fluoreszenzmarkierter Nanopartikel auf der Basis von PLGA untersucht, die mit unterschiedlichen Oberflächenmodifikationen versehen waren: i) unmodifiziertes PLGA, ii) mit Chitosan überzogenes PLGA (Chit.-PLGA) und iii) Chit.-PLGA mit Überzügen aus verschiedenen Phospholipiden (PL) (DPPC (100), DPPC:Chol. (85:15) und DPPC:DOTAP (92:8)). Die Proben wurden in einer Mischung aus ACN:NaOH extrahiert und anhand der Fluoreszenz quantitativ bestimmt. Als Effekt des Überzugs mit Phospholipiden drangen DPPC (100) und DPPC:DOTAP (92:8) stärker in die Haarfollikel ein als die übrigen getesteten Nanopartikel. Dieser Effekt wurde sowohl beim Schweineohr-Modell als auch bei den menschlichen Probanden beobachtet.

Da nur ein kleiner Teil, der auf die Haut aufgetragenen Nanopartikel in die Haarfollikel eindringt ist es für die transkutane Vakzinierung essentiell, die größtmögliche Wirkstoffmenge im Follikel zu erreichen. Aus

der Literatur ist bekannt, dass Nanopartikel, die mit Massage aufgetragen wurden tiefer in die Follikel eindringen verglichen mit einer Applikation ohne Massage. Unter Anwendung der neuen Quantifikationsmethode wurde untersucht, ob Applikationstechniken wie manuelle Massage oder Vibration die in den Haarfollikel aufgenommene Menge an Nanopartikeln steigern können. Fluoreszenzmarkierte PLGA Nanopartikel wurden mit folgenden Techniken auf das Schweineohr-Modell aufgetragen: i) ohne Massage, ii) mit manueller Massage mit dem behandschuhten Zeigefinger, iii) mit einem vibrierenden Massagegerät. Weder die manuelle Massage noch Massage mit einem vibrierenden Massagegerät waren in der Lage, die Menge an Nanopartikeln im Haarfollikel signifikant zu steigern.

Weiterhin konnte gezeigt werden, dass die Verwendung von Nanopartikeln als Arzneistoffträger, verglichen mit Lösungen die Wirkstoffmenge im Haarfollikel steigert. Im Schweineohr-Modell war die Menge an Ovalbumin im Haarfollikel 2 – 3-mal so hoch als bei der Verwendung einer Ovalbumin-Lösung. Zusätzlich kann die im Haarfollikel deponierte Wirkstoffmenge durch Auftragung größerer Mengen an Nanopartikeln um etwa den Faktor 2 – 2.4 gesteigert werden.

Für eine Machbarkeitsstudie wurden PLGA und Chitosan-PLGA Nanopartikel mit Ovalbumin als Modellantigen hergestellt. Ovalbumin wurde erfolgreich, mit nur einem moderaten Verlust an biologischer Aktivität in die Partikel eingearbeitet. In einer Zellkulturuntersuchung stimulierte das eingeschlossene Ovalbumin die Proliferation von CD4+ und CD8+-T-Zellen stärker als Ovalbumin-Lösung. Im adoptiven Zelltransfer wurde gezeigt, dass das Modellantigen Ovalbumin über die transfollikuläre Route appliziert werden kann. Dieses erste Experiment ist ein Machbarkeitsnachweis für die Applikation von Antigenen und gleichzeitige Stimulation Antigen spezifischer T-Zellen durch transfollikuläre Vakzinierung durch Nanopartikel als Trägersystem.

Zusammenfassend kann man die transfollikuläre Vakzinierung mit Nanopartikeln als Impfstoffträger als vielversprechenden Ansatz bezeichnen. Die größte Herausforderung besteht jedoch darin, eine

ausreichend große Menge an Antigen verabreichen zu können. Bislang geht der größte Teil des aufgetragenen Antigens auf der Hautoberfläche verloren. Obgleich erste Ergebnisse vielversprechend waren lässt sich dies nicht mit Konzepten zur Dosiseinsparung vereinbaren. Die weitere Forschung sollte sich darum auf die Optimierung von Trägersystemen konzentrieren um die Wirkstoffmenge im Haarfollikel steigern zu können.

Die Ergebnisse der Machbarkeitsstudie am Mausmodell waren vielversprechend. In vivo-Studien zur transfollikulären Vakzinierung sollten vom Modellantigen Ovalbumin zu klinisch genutzten Antigenen wie Grippeimpfstoffen ausgeweitet werden und auch in anderen Tiermodellen durchgeführt werden. Aufgrund der extrem höheren Haarfollikeldichte der Maus im Vergleich zum Menschen, ist das Mausmodell nur bedingt geeignet. Werden zugelassene Impfstoffe in Nanopartikel aus von der FDA zugelassenen Polymeren eingearbeitet wäre sogar die Durchführung von klinischen Studien am Menschen in naher Zukunft denkbar.

Die Quantifikationsmethode kann bei der Entwicklung von Trägersystemen mit gesteigertem Penetrationsvermögen in die Haarfollikel helfen. Die Untersuchung des Einflusses von Phospholipid-Überzügen war ein erster Schritt, die Aufnahme beeinflussende Parameter zu ermitteln. Die quantitative Bestimmung der aufgenommenen Menge an Nanopartikeln im Haarfollikel ist relevant zur Dosisbestimmung, nicht nur für transkutane Immunisierung sondern für den Haarfollikel betreffende Therapie im Allgemeinen. Werden arzneistoffbeladene Nanopartikel verwendet, können der Verbleib der Partikel und der des Arzneistoffs parallel bestimmt werden. Die Methode kann einfach mit etablierten Untersuchungsmethoden wie beispielsweise der Tape-stripping-Technik kombiniert werden. Dies ist vor allem dann von Interesse, wenn die Haarfollikel die eigentlichen Therapieziele sind. Tape-stripping ist bereits jetzt Bestandteil des Probenzugs und wird eingesetzt, um die Hautoberfläche von dort verbliebenen Nanopartikeln zu reinigen. Durch eine größere Anzahl durchgeführter Tesafilmabrisse

könnte so simultan zur Bestimmung der Penetration in die Haarfollikel ein Tiefenprofil von in das Stratum corneum eingedrungenem Arzneistoff erstellt werden. Vor allem die Entwicklung aber auch Bioequivalenzstudien von Therapeutika gegen Erkrankungen, die die Haarfollikel betreffen, wie beispielsweise Akne oder Haarausfall, können von dieser Methode profitieren.

REFERENCES

[1] G. Cevc, G. Blume, Lipid vesicles penetrate into intact skin owing to the transdermal osmotic gradients and hydration force, Biochim Biophys Acta, 1104 (1992) 226-232.

[2] T. Gratieri, U.F. Schaefer, L. Jing, M. Gao, K.H. Kostka, R.F. Lopez, M. Schneider, Penetration of quantum dot particles through human skin, J Biomed Nanotechnol, 6 (2010) 586-595.

[3] P.N. Gupta, V. Mishra, A. Rawat, P. Dubey, S. Mahor, S. Jain, D.P. Chatterji, S.P. Vyas, Non-invasive vaccine delivery in transfersomes, niosomes and liposomes: a comparative study, Int J Pharm, 293 (2005) 73-82.

[4] A. Paul, G. Cevc, B.K. Bachhawat, Transdermal immunisation with an integral membrane component, gap junction protein, by means of ultradeformable drug carriers, transfersomes, Vaccine, 16 (1998) 188-195.

[5] B. Geusens, M. Van Gele, S. Braat, S.C. De Smedt, M.C.A. Stuart, T.W. Prow, W. Sanchez, M.S. Roberts, N.N. Sanders, J. Lambert, Flexible nanosomes (SECosomes) enable efficient siRNA delivery in cultured primary skin cells and in the viable epidermis of ex vivo human skin, Adv Funct Mater, 20 (2010) 4077-4090.

[6] D. Mishra, P.K. Mishra, V. Dubey, M. Nahar, S. Dabadghao, N.K. Jain, Systemic and mucosal immune response induced by transcutaneous immunization using Hepatitis B surface antigen-loaded modified liposomes, Eur J Pharm Sci, 33 (2008) 424-433.

[7] J. Wang, J.H. Hu, F.Q. Li, G.Z. Liu, Q.G. Zhu, J.Y. Liu, H.J. Ma, C. Peng, F.G. Si, Strong cellular and humoral immune responses induced by transcutaneous immunization with HBsAg DNA-cationic deformable liposome complex, Exp Dermatol, 16 (2007) 724-729.

[8] S. Hansen, C.-M. Lehr, Nanoparticles for transcutaneous vaccination, Microbial Biotechnol, 5 (2012) 156-167.

[9] E.L. Romero, M.J. Morilla, Topical and mucosal liposomes for vaccine delivery, Wiley Interdiscip Rev Nanomed Nanobiotechnol, 3 (2011) 356-375.

[10] J.P. Ryman-Rasmussen, J.E. Riviere, N.A. Monteiro-Riviere, Penetration of intact skin by quantum dots with diverse physicochemical properties, Toxicological Sciences, 91 (2006) 159-165.

[11] A. Patzelt, H. Richter, F. Knorr, U. Schaefer, C.M. Lehr, L. Dahne, W. Sterry, J. Lademann, Selective follicular targeting by modification of the particle sizes, J Control Release, 150 (2011) 45-48.

[12] A. Mittal, A.S. Raber, U.F. Schaefer, S. Weissmann, T. Ebensen, K. Schulze, C.A. Guzman, C.M. Lehr, S. Hansen, Non-invasive delivery of nanoparticles to hair follicles: A perspective for transcutaneous immunization, Vaccine, (2013).

[13] U. Jacobi, K. Engel, A. Patzelt, M. Worm, W. Sterry, J. Lademann, Penetration of pollen proteins into the skin, Skin Pharmacol Physiol, 20 (2007) 297-304.

[14] H. Fan, Q. Lin, G.R. Morrissey, P.A. Khavari, Immunization via hair follicles by topical application of naked DNA to normal skin, Nat Biotechnol, 17 (1999) 870-872.

[15] D.S. Shaker, B.R. Sloat, U.M. Le, C.V. Lohr, N. Yanasarn, K.A. Fischer, Z. Cui, Immunization by application of DNA vaccine onto a skin area wherein the hair follicles have been induced into anagen-onset stage, Molecular therapy : the journal of the American Society of Gene Therapy, 15 (2007) 2037-2043.

[16] R.B. Baleeiro, K.H. Wiesmüller, Y. Reiter, B. Baude, L. Dähne, A. Patzelt, J. Lademann, J.A. Barbuto, P. Walden, Topical Vaccination with Functionalized Particles Targeting Dendritic Cells, Journal of Investigative Dermatology, (2013).

[17] B. Combadiere, A. Vogt, B. Mahe, D. Costagliola, S. Hadam, O. Bonduelle, W. Sterry, S. Staszewski, H. Schaefer, S. van der Werf, C. Katlama, B. Autran, U. Blume-Peytavi, Preferential amplification of CD8 effector-T cells after transcutaneous application of an inactivated influenza vaccine: a randomized phase I trial, PLoS ONE, 5 (2010) e10818.

[18] N. Otberg, A. Patzelt, U. Rasulev, T. Hagemeister, M. Linscheid, R. Sinkgraven, W. Sterry, J. Lademann, The role of hair follicles in the percutaneous absorption of caffeine, Br J Clin Pharmacol, 65 (2008) 488-492.

[19] J. Lademann, H. Richter, A. Teichmann, N. Otberg, U. Blume-Peytavi, J. Luengo, B. Weiss, U.F. Schaefer, C.M. Lehr, R. Wepf, W. Sterry, Nanoparticles--an efficient carrier for drug delivery into the hair follicles, Eur J Pharm Biopharm, 66 (2007) 159-164.

[20] S. Mitragotri, Mechanical disruption of skin barrier for vaccine delivery, Drug Delivery System, 27 (2012) 202-212.

[21] R.F. Lopez, J.E. Seto, D. Blankschtein, R. Langer, Enhancing the transdermal delivery of rigid nanoparticles using the simultaneous application of ultrasound and sodium lauryl sulfate, Biomaterials, 32 (2011) 933-941.

[22] P. Karande, S. Mitragotri, Transcutaneous immunization: An overview of advantages, disease targets, vaccines, and delivery technologies, Annual Review of Chemical and Biomolecular Engineering, 1 (2010) 175-201.

[23] J. Lisziewicz, E. Rosenberg, J. Lieberman, H. Jessen, L. Lopalco, R. Siliciano, B. Walker, F. Lori, Control of HIV despite the discontinuation of antiretroviral therapy [2], New England Journal of Medicine, 340 (1999) 1683-1684.

[24] L. Gudmundsdotter, B. Wahren, B.K. Haller, A. Boberg, U. Edback, D. Bernasconi, S. Butto, H. Gaines, N. Imami, F. Gotch, F. Lori, J. Lisziewicz, E. Sandstrom, B. Hejdeman, Amplified antigen-specific immune

responses in HIV-1 infected individuals in a double blind DNA immunization and therapy interruption trial, Vaccine, 29 (2011) 5558-5566.

[25] J. Lisziewicz, N. Bakare, S.A. Calarota, D. Bánhegyi, J. Szlávik, E. Újhelyi, E.R. Toke, L. Molnár, Z. Lisziewicz, B. Autran, F. Lori, Single DermaVir immunization: Dose-dependent expansion of precursor/memory T cells against all HIV antigens in HIV-1 infected individuals, PLoS ONE, 7 (2012).

[26] J. Williams, L. Fox-Leyva, C. Christensen, D. Fisher, E. Schlicting, M. Snowball, S. Negus, J. Mayers, R. Koller, R. Stout, Hepatitis A vaccine administration: comparison between jet-injector and needle injection, Vaccine, 18 (2000) 1939-1943.

[27] C. Mathei, P. Van Damme, A. Meheus, Hepatitis B vaccine administration: comparison between jet-gun and syringe and needle, Vaccine, 15 (1997) 402-404.

[28] J.D. Millar, L. Morris, A. Macedo Filho, T.M. Mack, W. Dyal, A.A. Medeiros, The introduction of jet injection mass vaccination into the national smallpox eradication program of Brazil, Tropical and Geographical Medicine, 23 (1971) 89-101.

[29] J. Abb, F. Deinhardt, J. Eisenburg, The risk of transmission of hepatitis B virus using jet injection in inoculation, Journal of Infectious Diseases, 144 (1981) 179.

[30] P.C. DeMuth, W.F. Garcia-Beltran, M.L. Ai-Ling, P.T. Hammond, D.J. Irvine, Composite dissolving microneedles for coordinated control of antigen and adjuvant delivery kinetics in transcutaneous vaccination, Adv Funct Mater, 23 (2013) 161-172.

[31] M. Singh, A. Chakrapani, D. O'Hagan, Nanoparticles and microparticles as vaccine-delivery systems, Expert Rev Vaccines, 6 (2007) 797-808.

[32] P.L. Mottram, D. Leong, B. Crimeen-Irwin, S. Gloster, S.D. Xiang, J. Meanger, R. Ghildyal, N. Vardaxis, M. Plebanski, Type 1 and 2 immunity following vaccination is influenced by nanoparticle size: Formulation of a model vaccine for respiratory syncytial virus, Molecular Pharmaceutics, 4 (2007) 73-84.

[33] F. Rancan, Q. Gao, C. Graf, S. Troppens, S. Hadam, S. Hackbarth, C. Kembuan, U. Blume-Peytavi, E. Ruhl, J. Lademann, A. Vogt, Skin penetration and cellular uptake of amorphous silica nanoparticles with variable size, surface functionalization, and colloidal stability, ACS nano, 6 (2012) 6829-6842.

[34] Y.F. Ma, Y. Zhuang, X.F. Xie, C. Wang, F. Wang, D.M. Zhou, J.Q. Zeng, L.T. Cai, The role of surface charge density in cationic liposome-promoted dendritic cell maturation and vaccine-induced immune responses, Nanoscale, 3 (2011) 2307-2314.

[35] L.H. Higa, P. Schilrreff, A.P. Perez, M.A. Iriarte, D.I. Roncaglia, M.J. Morilla, E.L. Romero, Ultradeformable archaeosomes as new topical adjuvants, Nanomedicine-Nanotechnology Biology and Medicine, 8 (2012) 1319-1328.

[36] T. Uto, T. Akagi, T. Hamasaki, M. Akashi, M. Baba, Modulation of innate and adaptive immunity by biodegradable nanoparticles, Immunology Letters, 125 (2009) 46-52.

[37] S.A. Frech, H.L. DuPont, A.L. Bourgeois, R. McKenzie, J. Belkind-Gerson, J.F. Figueroa, P.C. Okhuysen, N.H. Guerrero, F.G. Martinez-Sandoval, J.H.M. Meléndez-Romero, Z.-D. Jiang, E.J. Asturias, J. Halpern, O.R. Torres, A.S. Hoffman, C.P. Villar, R.N. Kassem, D.C. Flyer, B.H. Andersen, K. Kazempour, S.A. Breisch, G.M. Glenn, Use of a patch containing heat-labile toxin from Escherichia coli against travellers' diarrhoea: a phase II, randomised, double-blind, placebo-controlled field trial, The Lancet, 371 (2008) 2019-2025.

[38] R.K. Gupta, E.H. Relyveld, E.B. Lindblad, B. Bizzini, S. Benefraim, C.K. Gupta, Adjuvants - a Balance between Toxicity and Adjuvanticity, Vaccine, 11 (1993) 293-306.

[39] M. Diwan, P. Elamanchili, M. Cao, J. Samuel, Dose sparing of CpG oligodeoxynucleotide vaccine adjuvants by nanoparticle delivery, Curr Drug Deliv, 1 (2004) 405-412.

[40] K.D. Wilson, S.D. de Jong, Y.K. Tam, Lipid-based delivery of CpG oligonucleotides enhances immunotherapeutic efficacy, Adv. Drug Deliver. Rev., 61 (2009) 233-242.

[41] A. Bershteyn, M.C. Hanson, M.P. Crespo, J.J. Moon, A.V. Li, H. Suh, D.J. Irvine, Robust IgG responses to nanograms of antigen using a biomimetic lipid-coated particle vaccine, Journal of controlled release : official journal of the Controlled Release Society, 157 (2012) 354-365.

[42] S. Fischer, E. Schlosser, M. Mueller, N. Csaba, H.P. Merkle, M. Groettrup, B. Gander, Concomitant delivery of a CTL-restricted peptide antigen and CpG ODN by PLGA microparticles induces cellular immune response, Journal of Drug Targeting, 17 (2009) 652-661.

[43] E. Schlosser, M. Mueller, S. Fischer, S. Basta, D.H. Busch, B. Gander, M. Groettrup, TLR ligands and antigen need to be coencapsulated into the same biodegradable microsphere for the generation of potent cytotoxic T lymphocyte responses, Vaccine, 26 (2008) 1626-1637.

[44] S.M. Bal, S. Hortensius, Z. Ding, W. Jiskoot, J.A. Bouwstra, Co-encapsulation of antigen and Toll-like receptor ligand in cationic liposomes affects the quality of the immune response in mice after intradermal vaccination, Vaccine, 29 (2011) 1045-1052.

[45] N. Otberg, H. Richter, H. Schaefer, U. Blume-Peytavi, W. Sterry, J. Lademann, Variations of Hair Follicle Size and Distribution in Different Body Sites, Journal of Investigative Dermatology, 122 (2004) 14-19.

[46] Y. Frum, G.M. Eccleston, V.M. Meidan, In-vitro permeation of drugs into porcine hair follicles: is it quantitatively equivalent to permeation into human hair follicles?, J Pharm Pharmacol, 60 (2008) 145-151.

[47] J. Lademann, H. Richter, U.F. Schaefer, U. Blume-Peytavi, A. Teichmann, N. Otberg, W. Sterry, Hair follicles - A long-term reservoir for drug delivery, Skin Pharmacology and Physiology, 19 (2006) 232-236.

[48] A. Mittal, A.S. Raber, U.F. Schaefer, S. Weissmann, T. Ebensen, K. Schulze, C.A. Guzmán, C.M. Lehr, S. Hansen, Non-invasive delivery of nanoparticles to hair follicles: A perspective for transcutaneous immunization, Vaccine, in press (2013).

[49] H. Todo, E. Kimura, Y. Yasuno, Y. Tokudome, F. Hashimoto, Y. Ikarashi, K. Sugibayashi, Permeation pathway of macromolecules and nanospheres through skin, Biological and Pharmaceutical Bulletin, 33 (2010) 1394-1399.

[50] L.M. Lieb, A.P. Liimatta, R.N. Bryan, B.D. Brown, G.G. Krueger, Description of the intrafollicular delivery of large molecular weight molecules to follicles of human scalp skin in vitro, Journal of Pharmaceutical Sciences, 86 (1997) 1022-1029.

[51] P. Filipe, J.N. Silva, R. Silva, J.L. Cirne De Castro, M. Marques Gomes, L.C. Alves, R. Santus, T. Pinheiro, Stratum corneum is an effective barrier to TiO2 and ZnO nanoparticle percutaneous absorption, Skin Pharmacology and Physiology, 22 (2009) 266-275.

[52] P. Rolland, M.A. Bolzinger, C. Cruz, S. Briançon, D. Josse, Human scalp permeability to the chemical warfare agent VX, Toxicology in Vitro, 25 (2011) 1974-1980.

[53] G.M. Gelfuso, T. Gratieri, M.B. Delgado-Charro, R.H. Guy, R.F. Vianna Lopez, Iontophoresis-targeted, follicular delivery of minoxidil sulfate for the treatment of alopecia, J Pharm Sci, 102 (2013) 1488-1494.

[54] N. Banka, M.J. Bunagan, J. Shapiro, Pattern hair loss in men: diagnosis and medical treatment, Dermatol Clin, 31 (2013) 129-140.

[55] D. Thiboutot, Regulation of human sebaceous glands, J Invest Dermatol, 123 (2004) 1-12.

[56] J. Lademann, H. Richter, A. Teichmann, N. Otberg, U. Blume-Peytavi, J. Luengo, B. Weiss, U.F. Schaefer, C.M. Lehr, R. Wepf, W. Sterry, Nanoparticles - An efficient carrier for drug delivery into the hair follicles, Eur J Pharm Biopharm, 66 (2007) 159-164.

[57] A. Teichmann, U. Jacobi, M. Ossadnik, H. Richter, S. Koch, W. Sterry, J. Lademann, Differential stripping: determination of the amount of topically applied substances penetrated into the hair follicles, J Invest Dermatol, 125 (2005) 264-269.

[58] J. Lademann, H. Weigmann, C. Rickmeyer, H. Barthelmes, H. Schaefer, G. Mueller, W. Sterry, Penetration of titanium dioxide microparticles in a sunscreen formulation into the horny layer and the follicular orifice, Skin Pharmacol Appl Skin Physiol, 12 (1999) 247-256.

[59] H.I. Labouta, L.K. el-Khordagui, T. Kraus, M. Schneider, Mechanism and determinants of nanoparticle penetration through human skin, Nanoscale, 3 (2011) 4989-4999.

[60] O. Lee, S.H. Jeong, W.U. Shin, G. Lee, C. Oh, S.W. Son, Influence of surface charge of gold nanorods on skin penetration, Skin research and technology : official journal of International Society for Bioengineering and the Skin, 19 (2013) e390-396.

[61] T.W. Prow, J.E. Grice, L.L. Lin, R. Faye, M. Butler, W. Becker, E.M. Wurm, C. Yoong, T.A. Robertson, H.P. Soyer, M.S. Roberts, Nanoparticles and microparticles for skin drug delivery, Adv Drug Deliv Rev, (2011).

[62] G.W. Lu, S. Valiveti, J. Spence, C. Zhuang, L. Robosky, K. Wade, A. Love, L.Y. Hu, D. Pole, M. Mollan, Comparison of artificial sebum with human and hamster sebum samples, Int J Pharm, 367 (2009) 37-43.

[63] J. Schaefer, J. Sitterberg, C. Ehrhardt, M.N.V.R. Kumar, U. Bakowsky, A new drug vehicle - lipid coated biodegradable nanoparticles, Advances in Science and Technology, 57 (2008) 148-153.

[64] B. Weiss, U.F. Schaefer, J. Zapp, A. Lamprecht, A. Stallmach, C.-M. Lehr, Nanoparticles made of fluorescence-labelled poly(L-lactide-co-glycolide): Preparation, stability, and biocompatibility, Journal of Nanoscience and Nanotechnology, 6 (2006) 3048-3056.

[65] OECD, OECD Guideline for the testing of chemicals - Skin Absorption: in vitro method, (2004).

[66] J. Lademann, H.J. Weigmann, S. Schanzer, H. Richter, H. Audring, C. Antoniou, G. Tsikrikas, H. Gers-Barlag, W. Sterry, Optical investigations to avoid the disturbing influences of furrows and wrinkles quantifying penetration of drugs and cosmetics into the skin by tape stripping, J Biomed Opt, 10 (2005) 54015.

[67] Y. Xiao, M.R. Wiesner, Characterization of surface hydrophobicity of engineered nanoparticles, J Hazard Mater, 215-216 (2012) 146-151.

[68] V. Klang, J.C. Schwarz, A. Hartl, C. Valenta, Facilitating in vitro Tape Stripping: Application of Infrared Densitometry for Quantification of Porcine Stratum Corneum Proteins, Skin Pharmacol Physiol, 24 (2011) 256-268.

[69] L.M. Russell, S. Wiedersberg, M. Begona Delgado-Charro, The determination of stratum corneum thickness: An alternative approach, European Journal of Pharmaceutics and Biopharmaceutics, 69 (2008) 861-870.

[70] OECD, Test guideline 427: Skin Absorption: In Vivo Method, in, OECD, Paris, 2004.

[71] OECD, Test guideline 428: Skin Absorption: In Vitro Method, in, OECD, Paris, 2004.

[72] SCCNFP, Basic criteria for the in-vitro assessment of dermal absorption of cosmetic ingredients, in, 2003.

[73] J. Lademann, F. Knorr, H. Richter, U. Blume-Peytavi, A. Vogt, C. Antoniou, W. Sterry, A. Patzelt, Hair follicles--an efficient storage and penetration pathway for topically applied substances. Summary of recent results obtained at the Center of Experimental and Applied Cutaneous Physiology, Charite - Universitatsmedizin Berlin, Germany, Skin Pharmacol Physiol, 21 (2008) 150-155.

[74] U. Jacobi, M. Kaiser, R. Toll, S. Mangelsdorf, H. Audring, N. Otberg, W. Sterry, J. Lademann, Porcine ear skin: An in vitro model for human skin, Skin Research and Technology, 13 (2007) 19-24.

[75] O. Lee, S.H. Jeong, W.U. Shin, G. Lee, C. Oh, S.W. Son, Influence of surface charge of gold nanorods on skin penetration, Skin Res Technol, 19 (2013) e390-396.

[76] L. Redondo-Morata, M.I. Giannotti, F. Sanz, Influence of cholesterol on the phase transition of lipid bilayers: a temperature-controlled force spectroscopy study, Langmuir : the ACS journal of surfaces and colloids, 28 (2012) 12851-12860.

[77] A. Patzelt, H. Richter, F. Knorr, U. Schafer, C.M. Lehr, L. Dahne, W. Sterry, J. Lademann, Selective follicular targeting by modification of the particle sizes, J Control Release, 150 (2011) 45-48.

[78] G.M. Glenn, D.N. Taylor, X. Li, S. Frankel, A. Montemarano, C.R. Alving, Transcutaneous immunization: a human vaccine delivery strategy using a patch, Nat Med, 6 (2000) 1403-1406.

[79] S. Hansen, C.M. Lehr, Nanoparticles for transcutaneous vaccination, Microbial Biotechnology, 5 (2012) 156-167.

[80] B. Combadiere, B. Mahe, Particle-based vaccines for transcutaneous vaccination, Comp Immunol Microb, 31 (2008) 293-315.

[81] G.M. Glenn, R.T. Kenney, Mass vaccination: Solutions in the skin, Curr. Top. Microbiol., 304 (2006) 247-268.

[82] M. Schneider, F. Stracke, S. Hansen, U.F. Schaefer, Nanoparticles and their interactions with the dermal barrier, Dermatoendocrinol, 1 (2009) 197-206.

[83] A. Domashenko, S. Gupta, G. Cotsarelis, Efficient delivery of transgenes to human hair follicle progenitor cells using topical lipoplex, Nature biotechnology, 18 (2000) 420-423.

[84] Z. Yu, W.G. Chung, B.R. Sloat, C.V. Lohr, R. Weiss, B.L. Rodriguez, X. Li, Z. Cui, The extent of the uptake of plasmid into the skin determines the immune responses induced by a DNA vaccine applied topically onto the skin, J Pharm Pharmacol, 63 (2011) 199-205.

[85] H.J. Weigmann, J. Lademann, H. Meffert, H. Schaefer, W. Sterry, Determination of the horny layer profile by tape stripping in combination with optical spectroscopy in the visible range as a prerequisite to quantify percutaneous absorption, Skin Pharmacology and Applied Skin Physiology, 12 (1999) 34-45.

[86] M.D. Blanco, M.J. Alonso, Development and characterization of protein-loaded poly(lactide-co-glycolide) nanospheres, Eur J Pharm Biopharm, 43 (1997) 287-294.

[87] C. Schulze, U.F. Schaefer, C.A. Ruge, W. Wohlleben, C.M. Lehr, Interaction of metal oxide nanoparticles with lung surfactant protein A, Eur J Pharm Biopharm, 77 (2011) 376-383.

[88] C. Liard, S. Munier, M. Arias, A. Joulin-Giet, O. Bonduelle, D. Duffy, R.J. Shattock, B. Verrier, B. Combadiere, Targeting of HIV-p24 particle-based vaccine into differential skin layers induces distinct arms of the immune responses, Vaccine, 29 (2011) 6379-6391.

[89] B. Mahe, A. Vogt, C. Liard, D. Duffy, V. Abadie, O. Bonduelle, A. Boissonnas, W. Sterry, B. Verrier, U. Blume-Peytavi, B. Combadiere, Nanoparticle-based targeting of vaccine compounds to skin antigen-

presenting cells by hair follicles and their transport in mice, The Journal Of Investigative Dermatology, 129 (2009) 1156-1164.

[90] P.E. Taylor, K.W. Jacobson, J.M. House, M.M. Glovsky, Links between pollen, atopy and the asthma epidemic, International Archives of Allergy and Immunology, 144 (2007) 162-170.

[91] J.W. Streilein, L.W. Lonsberry, P.R. Bergstresser, Depletion of epidermal langerhans cells and Ia immunogenicity from tape-stripped mouse skin, J Exp Med, 155 (1982) 863-871.

[92] A.C. Gilliam, I.B. Kremer, Y. Yoshida, S.R. Stevens, E. Tootell, M.B. Teunissen, C. Hammerberg, K.D. Cooper, The human hair follicle: a reservoir of CD40+ B7-deficient Langerhans cells that repopulate epidermis after UVB exposure, J Invest Dermatol, 110 (1998) 422-427.

[93] R.K. Gupta, M. Singh, D.T. O'Hagan, Poly(lactide-co-glycolide) microparticles for the development of single-dose controlled-release vaccines, Advanced Drug Delivery Reviews, 32 (1998) 225-246.

[94] M. Amidi, E. Mastrobattista, W. Jiskoot, W.E. Hennink, Chitosan-based delivery systems for protein therapeutics and antigens, Advanced Drug Delivery Reviews, 62 (2010) 59-82.

[95] S.S. Pai, R.D. Tilton, T.M. Przybycien, Poly(ethylene glycol)-Modified Proteins: Implications for Poly(lactide-co-glycolide)-Based Microsphere Delivery, Aaps Journal, 11 (2009) 88-98.

[96] S. Taetz, N. Nafee, J. Beisner, K. Piotrowska, C. Baldes, T.E. Murdter, H. Huwer, M. Schneider, U.F. Schaefer, U. Klotz, C.M. Lehr, The influence of chitosan content in cationic chitosan/PLGA nanoparticles on the delivery efficiency of antisense 2'-O-methyl-RNA directed against telomerase in lung cancer cells, Eur J Pharm Biopharm, 72 (2009) 358-369.

[97] S. Mao, W. Sun, T. Kissel, Chitosan-based formulations for delivery of DNA and siRNA, Advanced Drug Delivery Reviews, 62 (2010) 12-27.

[98] C.-M. Lehr, J.A. Bouwstra, E.H. Schacht, H.E. Junginger, In vitro evaluation of mucoadhesive properties of chitosan and some other natural polymers, International Journal of Pharmaceutics, 78 (1992) 43-48.

[99] S.M. Bal, B. Slutter, E. van Riet, A.C. Kruithof, Z. Ding, G.F. Kersten, W. Jiskoot, J.A. Bouwstra, Efficient induction of immune responses through intradermal vaccination with N-trimethyl chitosan containing antigen formulations, J Control Release, 142 (2010) 374-383.

[100] M. Friede, M.T. Aguado, Need for new vaccine formulations and potential of particulate antigen and DNA delivery systems, Advanced Drug Delivery Reviews, 57 (2005) 325-331.

[101] Y. Men, C. Thomasin, H.P. Merkle, B. Gander, G. Corradin, A Single Administration of Tetanus Toxoid in Biodegradable Microspheres Elicits T-Cell and Antibody-Responses Similar or Superior to Those Obtained with Aluminum Hydroxide, Vaccine, 13 (1995) 683-689.

[102] Y. Ogawa, H. Okada, T. Heya, T. Shimamoto, Controlled Release of Lhrh Agonist, Leuprolide Acetate, from Microcapsules - Serum Drug Level Profiles and Pharmacological Effects in Animals, J Pharm Pharmacol, 41 (1989) 439-444.

[103] P. Riesz, T. Kondo, Free radical formation induced by ultrasound and its biological implications, Free Radic Biol Med, 13 (1992) 247-270.

[104] A.S. Determan, J.H. Wilson, M.J. Kipper, M.J. Wannemuehler, B. Narasimhan, Protein stability in the presence of polymer degradation products: Consequences for controlled release formulations, Biomaterials, 27 (2006) 3312-3320.

[105] M.L. Ye, S. Kim, K. Park, Issues in long-term protein delivery using biodegradable microparticles, Journal of Controlled Release, 146 (2010) 241-260.

[106] G. Crotts, T.G. Park, Stability and release of bovine serum albumin encapsulated within poly(D,L-lactide-co-glycolide) microparticles, Journal of Controlled Release, 44 (1997) 123-134.

[107] J. Banchereau, R.M. Steinman, Dendritic cells and the control of immunity, Nature, 392 (1998) 245-252.

[108] M.S. Maddur, J. Vani, J.D. Dimitrov, Kithiganahalli N. Balaji, S. Lacroix-Desmazes, S.V. Kaveri, J. Bayry, Dendritic Cells in Autoimmune Diseases, The Open Arthritis Journal, (2010) 1-7.

[109] Y.Y. Lan, Z.L. Wang, G. Raimondi, W.H. Wu, B.L. Colvin, A. De Creus, A.W. Thomson, "Alternatively activated" dendritic cells preferentially secrete IL-10, expand Foxp3(+)CD4(+) T cells, and induce long-term organ allograft survival in combination with CTLA4-Ig, J Immunol, 177 (2006) 5868-5877.

[110] S.S. Iyer, A.A. Ghaffari, G. Cheng, Lipopolysaccharide-Mediated IL-10 Transcriptional Regulation Requires Sequential Induction of Type I IFNs and IL-27 in Macrophages, J Immunol, 185 (2010) 6599-6607.

[111] O. Harush-Frenkel, N. Debotton, S. Benita, Y. Altschuler, Targeting of nanoparticles to the clathrin-mediated endocytic pathway, Biochemical and biophysical research communications, 353 (2007) 26-32.

[112] C. Keijzer, B. Slutter, R. van der Zee, W. Jiskoot, W. van Eden, F. Broere, PLGA, PLGA-TMC and TMC-TPP nanoparticles differentially modulate the outcome of nasal vaccination by inducing tolerance or enhancing humoral immunity, PLoS ONE, 6 (2011) e26684.

[113] B. Slutter, L. Plapied, V. Fievez, M.A. Sande, A. des Rieux, Y.J. Schneider, E. Van Riet, W. Jiskoot, V. Preat, Mechanistic study of the adjuvant effect of biodegradable nanoparticles in mucosal vaccination, Journal of controlled release : official journal of the Controlled Release Society, 138 (2009) 113-121.

[114] M. Yoshida, J.E. Babensee, Molecular aspects of microparticle phagocytosis by dendritic cells, Journal of biomaterials science. Polymer edition, 17 (2006) 893-907.

[115] S. Fischer, E. Uetz-von Allmen, Y. Waeckerle-Men, M. Groettrup, H.P. Merkle, B. Gander, The preservation of phenotype and functionality of dendritic cells upon phagocytosis of polyelectrolyte-coated PLGA microparticles, Biomaterials, 28 (2007) 994-1004.

[116] K.A. Pape, E.R. Kearney, A. Khoruts, A. Mondino, R. Merica, Z.-M. Chen, E. Ingulli, J. White, J.G. Johnson, M.K. Jenkins, Use of adoptive transfer of T-cell antigen-receptor-transgenic T cells for the study of T-cell activation in vivo, Immunological Reviews, 156 (1997) 67-78.

[117] E. Proksch, J. Brasch, W. Sterry, Integrity of the permeability barrier regulates epidermal Langerhans cell density, Br J Dermatol, 134 (1996) 630-638.

[118] G. Mattheolabakis, G. Lagoumintzis, Z. Panagi, E. Papadimitriou, C.D. Partidos, K. Avgoustakis, Transcutaneous delivery of a nanoencapsulated antigen: induction of immune responses, Int J Pharm, 385 (2010) 187-193.

[119] OECD, Guidance document for the conduct of skin absorption studies. OECD Series on Testing and Assessment. No 28, in, Environment Directorate, Paris, 2004.

[120] S. Mangelsdorf, N. Otberg, H.I. Maibach, R. Sinkgraven, W. Sterry, J. Lademann, Ethnic variation in vellus hair follicle size and distribution, Skin Pharmacol Physiol, 19 (2006) 159-167.

[121] S. Mangelsdorf, Comparative evaluation of skin physiological parameters which inlfuence percutaneous penetration in different animal species, in: Insitute for animal physiology, Free University Berlin, Berlin, 2006.

[122] R.L. Bronaugh, R.F. Stewart, E.R. Congdon, Methods for in vitro percutaneous absorption studies. II. Animal models for human skin, Toxicology and Applied Pharmacology, 62 (1982) 481-488.

[123] A. Patzelt, H. Richter, R. Buettemeyer, H.J. Huber, U. Blume-Peytavi, W. Sterry, J. Lademann, Differential stripping demonstrates a significant reduction of the hair follicle reservoir in vitro compared to in vivo, Eur J Pharm Biopharm, 70 (2008) 234-238.

[124] R. Toll, U. Jacobi, H. Richter, J. Lademann, H. Schaefer, U. Blume-Peytavi, Penetration profile of microspheres in follicular targeting of terminal hair follicles, J Invest Dermatol, 123 (2004) 168-176.

[125] V.M. Meidan, M.C. Bonner, B.B. Michniak, Transfollicular drug delivery--is it a reality?, International Journal of Pharmaceutics, 306 (2005) 1-14.

ABBREVIATIONS

ACN	Acetonitrile
APC	Antigen presenting cell
BSA	Bovine serum albumin
cART	Combination antiretroviral therapie
CD 4/ CD 8	Clusters of differentiation (4 or 8)
CFSE	Carboxyfluoresceine succinimidyl ester
Chit-PLGA	Chitosan-PLGA
Chol.	Cholesterol
dd	double distilled
DC	Dendritic cell
DNA	Deoxyribonucleic acid
DPPC	Dipalmitoylphosphatidylcholine
DOTAP	1,2-Dioleoyl-3-trimethylammonium-propan
ELISA	Enzyme linked immuno assay
ESEM	Environmental scanning electron microscopy
FACS	Fluorescence activated cell sorting
FITC	Fluorescein isothiocynate
GRAS	Generally regarded as safe
HIV	Human immunodeficiency virus
HPLC UV/MS	high performance liquid chromatography ultraviolet/ mass spectroscopy
IQR	Interquartile range
ivivc	in vitro in vivo correlation
LC	Langerhans cell

LLOD	Lower limit of detection
LLOQ	Lower limit of quantification
LPS	Lipopolysaccharide
LSM	laser scanning microscopy
LT	E. coli heat labile toxine
MFI	Mean fluorescence intensity
MHC	Major Histocompatibility Complex
MP	Microparticle
NaOH	Sodium hydroxide
NP	Nanoparticle
OECD	Organisation for Economic Co-operation and Development
OVA	Ovalbumin
PBS	Phosphate buffer saline
PDI	Polydispersity index
PLGA	Poly lactide-co-glcolide
PVA	Polyvinyl alcohol
ROI	Region of interest
SC	Stratum corneum
SCCNFP	Scientific Committee on Cosmetic Products and Non-food products
SD	Standard deviation
SDS PAGE	Sodium dodecyl sulfate polyacrylamide gel electrophoresis
SEM	Scanning electron microscopy
SEM	Standard error mean
TCI	Transcutaneous Immunization
TCR	T-cell receptor
TEM	Transmission electron microscopy

TEWL	Transepidermal water loss
WHO	World Health Organization

LIST OF PUBLICATIONS

PUBLICATIONS IN PEER-REVIEWED JOURNALS

A. S. Raber, A. Mittal, J. Schäfer, U. Bakowsky, J. Reichrath, T. Vogt, U. F. Schaefer, S. Hansenand C.-M. Lehr; Quantification of nanoparticle uptake into hair follicles in pig ear and human forearm; Journal of controlled release 179 (2014) 25 - 32

A. Mittal[#], A. S. Raber[#] and S. Hansen Particle based vaccine formulations for transcutaneous immunization; Human Vaccine and Immunotherapeutics 9 (2013) 1950 - 1955

A. Mittal[#], A. S. Raber[#] , U.F. Schäfer, S. Weissmann, T.Ebensen, K. Schulze, C. A. Guzmán, C.-M. Lehr. and S. Hansen; Non-invasive delivery of nanoparticles to hair follicles – a perspective for transcutaneous immunization; Vaccine 31 (2013) 3442 – 3451

the authors contributed equaliy to the publication

CONFERENCE CONTRIBUTIONS

Poster presentations

A. Paulus, Schäfer U.F., C.-M. Lehr and S. Hansen, Visualization of fluorescent nanoparticles on pig ear skin, Jahrestagung der Gesellschaft für Dermopharmazie, 04.04. – 06.04.2011, Vaals, Netherlands

S. Hansen, A. Mittal, **A. Paulus**, C.A. Guzman, C.-M. Lehr: Nanoparticles for transcutaneous vaccination, HIPS Symposium, 16.06.2011, Saarbrücken, Germany.

A. S. Raber, A. Mittal, C.-M.Lehr and S. Hansen, Tissue based screening tools for the testing of follicular penetration of nanoparticles, Perspectives in Percutaneous Penetration conference, 10.04. – 14.04.2012

S. Hansen, A. Mittal, **A. S.Raber**, C.A. Guzman, C.-M. Lehr: Nanoparticles for transcutaneous vaccination, HIPS Symposium, 28.06.2012, Saarbrücken, Germany.

A. S. Raber, A. Mittal, C.-M.Lehr and S. Hansen, Tissue based screening tools for the testing of follicular penetration of nanoparticles, Dechema Jahrestagung, 10.09. – 13.09.2012, Karlsruhe, Germany

A. S. Raber, A. Mittal, Lehr C.-M., Tissue based screening tools for the testing of follicular penetration of nanoparticles, International Conference and Workshop on Biological Barriers, 29.02. – 09.03.2013, Saarbruecken, Germany

A. S. Raber, A. Mittal, J. Schäfer, U. Bakowsky, J. Reichrath, T. Voigt, T. Vogt, U.F. Schäfer, C.-M. Lehr and S. Hansen, In vitro - in vivo correlation of nanoparticle uptake into hair follicles, Jahrestagung der Gesellschaft für Dermopharmazie, 21.03. – 23.03.2013, Mainz, Germany

S. Hansen, A. Mittal, **A.S. Raber**, U.F. Schaefer, T. Ebensen, K. Schulze, C.A. Guzmán, C.M. Lehr, Non-invasive delivery of nanoparticles to hair follicles for transcutaneous vaccination, HIPS symposium, 18.07.2013 Saarbrücken, Germany.

A. S. Raber, A. Mittal, U. F. Schäfer, C.-M. Lehr, S. Hansen, Quantification of Nanoparticle uptake into hair follicles, Annual meeting of the controlled release society, 21.07. – 24.07.2013, Honolulu, USA

Oral presentations

A. Raber, A. Mittal, U.F. Schäfer, C-M. Lehr, S.Hansen, Transfollicular vaccination with nanoparticles- Is it possible?, Perspectives in Percutaneous Penetration conference, 10.04. – 14.04.2012

A. S. Raber, A. Mittal, J. Schäfer, U. Bakowsky, J. Reichrath, T. Voigt, U. F. Schäfer, C.-M. Lehr and S. Hansen, In vitro - in vivo correlation of nanoparticle uptake into hair follicles Jahrestagung der Gesellschaft für Dermopharmazie, 21.03. – 23.03.2013, Mainz, Germany

Awards

A. S. Raber, A. Mittal, Lehr C.-M., Tissue based screening tools for the testing of follicular penetration of nanoparticles, International Conference and Workshop on Biological Barriers, 29.02. – 09.03.2013, Saarbruecken, Germany, Poster award

A. S. Raber, A. Mittal, J. Schäfer, U. Bakowsky, J. Reichrath, T. Voigt, U. F. Schäfer, C.-M. Lehr and S. Hansen, In vitro - in vivo correlation of nanoparticle uptake into hair follicles Jahrestagung der Gesellschaft für Dermopharmazie, 21.03. – 23.03.2013, Mainz, Germany, Hans-Christian Korting Nachwuchspreis für Dermopharmazie 2013

DANKSAGUNG

Ich bedanke mich herzlich bei Professor Claus-Michael Lehr für die Überlassung des interessanten Promotionsthemas und die Aufnahme in die Arbeitsgruppe des Instituts.

Ich danke Herrn Professor Vogt für die Anfertigung des Zweitgutachtens, sowie allen Mitgliedern der Prüfungskommission.

Ich möchte mich vor allem bei Frau Dr. Steffi Hansen bedanken, die meine Arbeit direkt betreut hat. In einer hart aber herzlichen Zeit habe ich viel gelernt und viel gelacht und meine Promotion wurde auch noch aus der Ferne weiterbetreut.

Ich bedanke mich außerdem ganz herzlich bei Herrn apl. Professor Ulrich Schäfer. Er war stets um das Wohlergehen seiner Schäflein bemüht und stand mir mit enormer Fachkompetenz mit Rat und Tat zur Seite, sogar über den Ruhestand hinaus.

Ich bedanke mich bei Herrn Prof. Reichrath für die Unterstützung als Studienarzt und die gute Zusammenarbeit.

Danke an die Mitarbeiter des Teams von Professor Guzman am HZI in Braunschweig für die Durchführung der Zell- und Mäuseversuche. Besonderer Dank gebührt an dieser Stelle meinem Mitdoktoranden Ankit Mittal, der die erforderlichen Nanopartikel herstellte und die Experimente in zahllosen Braunschweig-Trips durchführte.

Bei Professor Udo Bakowsky und Herrn Dr. Jens Schäfer möchte ich mich für die Herstellung und Charakterisierung der Lipid gecoateten Nanopartikel bedanken.

Vielen Dank an Herrn Dr. Marcus Koch vom INM für die Anfertigung der ESEM Aufnahmen, die gute Zusammenarbeit und endlose Geduld beim Beantworten meiner Fragen.

Danke an die Firma Emil Färber und Co. KG in Zweibrücken für die Zurverfügungstellung der Schweineohren und an die Firma Uhu GmbH und Co KG für die Spende des Sekundenklebers.
Bei Christiane Mathes möchte ich mich für das Anfertigen der Cryo-Schnitte und bei Dominik Selzer für die Hilfe bei der statistischen Auswertung bedanken. Außerdem danke ich meinen tapferen Probanden, die ihre Zeit und Unterarme für die in vivo-Studie zur Verfügung stellten: Lutz, Simon, Chiara, Christiane, Nico, Christian, Emad und Julia.
Ich danke meinen Mitstreitern im Team „Steffi“ und meinen Kollegen im Hautlabor: Christina, Chrissi, Salem, Tsambika, Ana, Lutz, Hagar und Simon.
Ich bedanke mich herzlich bei Professor Marc Schneider, Dr. Hagar Labouta, und Leon Muijs für die Einweisung, Hilfe und Diskussionen rund um die Konfokalmikroskpie.
Vielen Dank auch den Technikern, Isabelle und Sarah. Viele Probleme konnten durch einen Besuch im Techniker-Büro oder im Chef-Vorzimmer gelöst werden.
Ein besonderer Dank gebührt meinen Büro-Mädels Sandra, Christina und Julia (ich rechne dich als erweiterte Bürodame einfach dazu) sowie meinem langjährigen Weggefährten Clemens. Danke, dass ihr mit mir Freud und Leid geteilt habt und für die vielen guten Gespräche vor allem abends oder bei geschlossener Bürotür.
Ich danke allen Kollegen am Institut. Es war eine schöne Zeit mit euch und ich schulde bestimmt jedem einzelnen von euch für irgendetwas meinen Dank.

Meiner Familie und vor allem meinem Mann danke ich für alles was man mit Geld nicht bezahlen und mit Worten nicht beschreiben kann. Mein Mann hat sicherlich einen ebenso großen Anteil am Gelingen dieser Arbeit wie ich selbst.

Danke!